Kaunas University of Technology

Faculty of Mechanical Engineering and Design

Fast Fading Model Effects in Vehicular Ad-Hoc Network

Master's Final Degree Project

Govardhan Seshasayee

Project author

Assoc. prof. Saulius Japertas

Supervisor

Kaunas, 2022

Kaunas University of Technology

Faculty of Mechanical Engineering and Design

Fast Fading Effects Model in Vehicular Ad-Hoc Network

Master's Final Degree Project

Vehicle Engineering (6211EX021)

Govardhan Seshasayee

Project author

Assoc. prof. Saulius Japertas

Supervisor

Assoc. prof. Vitas Grimaila.

Reviewer

Kaunas, 2022

Kaunas University of Technology

Faculty of Mechanical Engineering and Design

Govardhan Seshasayee

Fast Fading Effects Model in Vehicular Ad-Hoc Networks

Declaration of Academic Integrity

I confirm the following:

1. I have prepared the final degree project independently and honestly without any violations of the copyrights or other rights of others, following the provisions of the Law on Copyrights and Related Rights of the Republic of Lithuania, the Regulations on the Management and Transfer of Intellectual Property of Kaunas University of Technology (hereinafter – University) and the ethical requirements stipulated by the Code of Academic Ethics of the University;

2. All the data and research results provided in the final degree project are correct and obtained legally; none of the parts of this project are plagiarised from any printed or electronic sources; all the quotations and references provided in the text of the final degree project are indicated in the list of references;

3. I have not paid anyone any monetary funds for the final degree project or the parts thereof unless required by the law;

4. I understand that in the case of any discovery of the fact of dishonesty or violation of any rights of others, the academic penalties will be imposed on me under the procedure applied at the University; I will be expelled from the University and my final degree project can be submitted to the Office of the Ombudsperson for Academic Ethics and Procedures in the examination of a possible violation of academic ethics.

Govardhan Seshasayee

Confirmed electronically

Kaunas University of Technology

Faculty of Mechanical Engineering and Design

Study programme: Vehicle Engineering (6211EX021)

Task of the Master's Final Degree Project

Given to the student: *Govardhan Seshasayee*

1. Title of the Project: Fast Fading Effects Model in Vehicular Ad-Hoc Networks. Greitai blėstantis modelis, efektai transporto priemonių ad-hoc tinkluose.

2. Aim of the Project: To develop a model that include the effects of fast-fading and evaluate the model for the accuracy to perform and experiment for valuation of fast-fading considering various scenarios.

3. Tasks of the Project: Tasks to reach aim of the project. To perform literature analysis of different journals for the development of a model with fast fading effects. To obtain datasets from literature for model evaluation. To analyse the model using the data obtained by performing experiments to estimate the error rate of the model. To get the desirable distances at which the amplitude dominant signal is to be considered by working on different scenarios to obtain the final model and its dependency on the distance.

4. Structure of the Text Part:

Introduction
I. Literature Survey
II. Methodology
III. Theoretical Model
IV. Experimentation
V. Results and Discussion
Conclusion
Reference
Appendix

5. Consultants of the Project:

Author of the Final Degree Project	Govardhan Seshasayee
	(name, surname, date)
Supervisor of the Final Degree Project	Assoc. prof. Saulius Japertas
	(Abbreviation of the position, name, surname, date)
Head of Study Programmes	Assoc. prof. Saulius Japertas
	(abbreviation of the position, name, surname, date)

Govardhan Seshasayee. Fast fading model, effects in Vehicular Ad-hoc Networks. Master's Final Degree Project / supervisor Assoc. prof. Saulius Japertas; Faculty of Mechanical Engineering and Design, Kaunas University of Technology.

Study field and area (study field group): Transport Engineering (E12), Engineering Science.

Keywords: VANET's, Fast fading, Shadow fading, Path Loss, InSSIDer.

Kaunas, 2022. p.59.

Summary

Vehicular Ad-hoc Networks are analogous to Mobile ad-hoc networks but are dedicated to vehicles. There are dedicated short range communication system which have potential of transferring information between various vehicles and road-side infrastructure. They are otherwise called Intelligent Transport Networks which comes under the Intelligent Transport Systems (ITS) otherwise can also be called as Internet of vehicles. These are one-hop and multi-hop communication systems which have applications in various fields. In this study the fast-fading effects which is caused by the speedy changes in phase and amplitude of the received signal in the receiver was research. Currently, VANET network radio signal prediction models such as log-normal shadowing, Nakagami fading, Rayleigh, Rician fading model, etc., does not include the fast-fading effects. In this work, these models were analysed, and a log-normal model was chosen to create a mathematical model that also estimates rapid inhibition. The validation of the developed mathematical model was initially performed on the basis of two scientific papers and later verified and corrected in experiments. The experiments were performed according to three scenarios using a Wi-Fi access point and signal measurement with the help of InSSIDer. InSSIDer is a Wi-Fi network scanner software that graphically and digitally displays signal strength over time. A 2.45 GHz mobile phone public Internet access point with a transmission power of 10 dBm was used as the signal source. The received signal strength obtained from the InSSIDer is used to calculate the pathloss, shadowing and the fast-fading effects. The accuracy is primarily checked by optimising the signal source in the open area and then by placing the signal inside the car after which there is a distortion in the signal strength obtained is observed, the error rate was calculated and the gaussian normal distribution was used on the path loss and the shadowing effect with respect to the pathloss was plotted. The error rate in the measured values were observed at a maximum of 10 % with an average of 3.05% out of the 60 readings performed for the accuracy score experimentally. This error is observed as the experimental error. The model accuracy of 96.95% taking in account the average of the error rate is achieved. Such good accuracy of the model was also confirmed by experiments under three scenarios. It has been found that at short distances up to 50 m, signal fading is affected by both slow and fast fading, and at distances greater than 50 m, slow fading is predominant. So, the model is concluded as such:

$$L_p = \begin{cases} L_p(d_0) + 10nlg\left(\frac{d}{d_0}\right) + N_\sigma(0,\sigma) + N_F(\alpha,\sigma), & if\ d \le 50\ m \\ L_p(d_0) + 10nlg\left(\frac{d}{d_0}\right) + 2N_\sigma(0,\sigma) & if\ d > 50\ m \end{cases}$$

Govardhan Seshasayee. Greitai blėstantis modelis, efektai transporto priemonių ad-hoc tinkluose. Magistro baigiamasis projektas / supervisor Assoc. prof. Saulius Japertas; Kauno technologijos universitetas, Mechanikos inžinerijos ir dizaino fakultetas.

Studijų kryptis ir sritis (studijų krypčių grupė): Transporto inžinerija (E12), Inžinerijos mokslai.

Reikšminiai žodžiai: VANET, greitas blukimas, šešėlių išnykimas, kelio praradimas, InSSIDer.

Kaunas, 2022. p.59

Santrauka

Transporto Ad-hoc tinklai yra analogiški mobiliesiems Ad-hoc tinklams, bet yra skirti transporto priemonėms. Tai speciali trumpo nuotolio ryšio sistema, galinti keistis informacija tarp įvairių transporto priemonių ir kelių infrastruktūros. Tokie tinklai kitaip vadinami išmaniaisiais transporto tinklais, kurie patenka į intelektualiąsias transporto sistemas (ITS). Tokie tinklai taip pat gali būti vadinami transporto priemonių internetu. Tai yra vieno radijo ryšio (angl. – radio hop) ir kelių radijo ryšių sistemos, kurios taikomos įvairiose srityse. Šiame darbe buvo tiriamas greitas signalo slopimo (angl. – fast fading) efektas, kurį sukelia greiti priimamo signalo fazės ir amplitudės pokyčiai imtuve. Šiuo metu VANET tinklo ryšio prognozavimo modeliai, pvz., log-normalus šešėliavimas, Nakagami, Rayleigh, Rician ir kt., neapima greito slopinimo efektų. Šiame darbe šie modeliai buvo analizuojami, o log-normalus modelis buvo pasirinktas norint sukurti matematinį modelį, įvertinantį ir greitą slopinimą. Sukurto matematinio modelio korektiškumo patvirtinimas pradžioje buvo atliktas remiantis dviem moksliniais darbais, o vėliau patikrintas ir pakoreguotas atliekant eksperimentus. Eksperimentai buvo atlikti pagal tris scenarijus panaudojant WiFi prieigos tašką ir signalą matuojant „InSSIDer“ pagalba. „InSSIDer“ yra „Wi-Fi“ tinklo skaitytuvo programinė įranga, grafiškai ir skaitmeniu būdu atvaizduojanti signalo stiprumą laikui bėgant. Kaip signalo šaltinis buvo naudojamas 2,45 GHz dažnio mobiliojo telefono viešosios interneto prieigos taškas, kurio perdavimo galia buvo 10 dBm. Gautas signalo stiprumas iš InSSIDer, naudojamas apskaičiuojant kelio nuostolius, šešėliavimo ir greitai slopstančius efektus. Eksperimento tikslumas buvo pirmiausia tikrinamas lokalizuojant signalo šaltinį atviroje vietoje, o po to įdedant šį šaltinį į automobilio vidų, po kurio stebimas gauto signalo stiprumo kitimai, apskaičiuojamas paklaidų lygis, naudojamas Gauso normalusis skirstinys. Išmatuotų verčių paklaidų lygis buvo ne didesnis kaip 10 %, o vidutiniškai 3,05 % pagal 60 rodmenų. Ši paklaida laikoma eksperimentine paklaida. Pasiekiamas 96,95% modelio tikslumas, atsižvelgiant į klaidų lygio vidurkį. Tokį gerą modelio tikslumą taip pat patvirtino eksperimentai pagal tris scenarijus. Buvo nustatyta, kad trumpais atstumais iki 50 m signalo slopinimui turi įtaką tiek lėtas, tiek greitas slopinimas, o didesniems nei 50 m atstumams vyraujančią įtaką daro lėtas slopinimas. Tyrimų rezultate yra siūlomas toks modelis:

$$L_p = \begin{cases} L_p(d_0) + 10nlg\left(\frac{d}{d_0}\right) + N_\sigma(0,\sigma) + N_F(\alpha,\sigma), & if\ d \le 50\ m \\ L_p(d_0) + 10nlg\left(\frac{d}{d_0}\right) + 2N_\sigma(0,\sigma) & if\ d > 50\ m \end{cases}.$$

Table of Contents

List of Figures

List of Tables

Introduction

Vehicular Ad-hoc Networks (VANET) is the technology which applies the concepts of Mobile Ad-hoc Networks which is analogous to the creation of wireless networks to the vehicles by which there exists communication between the vehicles. The VANET's, were developed for network communication between the vehicles and the roadside which can improve the driving experience.

Smart cities have been the talk for quite a long time now which brings in the use of VANET's and its telecommunication between the city's infrastructure and safety. The VANET's build a communication network for vehicle - vehicle and vehicle – roadside which has a variety of benefits such as giving information to the road users and the traffic controllers. The road users have a benefit of better drivability as there is a constant communication amidst the vehicles which can make the people understand the road more easily. These networks can even go to an extent where it can intimate the drivers to brake when necessary and to control the speed at which the vehicles go which is achieved by the communication that is established in the vehicles. This network is highly capable of decreasing the fatality that occurs in the road and can be very useful in also identifying traffic violation as data of the communication between the vehicles are stored. When there exists some dangerous situation in certain part of the road it can intimate the drivers who use the road earlier so that the user can plan for rerouting which can reduce the travel time.

These communication in these techs are achieved using the network connections such as, GSM, LTE, 5G technologies etc., which is used in the vehicle and an information centre where the information is processed with a Wi-Fi or other networks. This is used to process the information is and send back the received signal and the data to the vehicle for effective operation. Many autonomous vehicles can be controlled and manipulated easily which results in lesser accidents and safer roads which are also a part of the sustainable transport system. As there is an increasing trend in the improvement of autonomous driving vehicles the development of these technologies will further improve the roads safety. The implementation has challenges like, high mobility, fading, and shadowing effects that act upon the communications which brings up the question of effective communication without data losses as most cars are moving at high speeds and tend to change their positions, and the major challenge of many participants in the road which can cause discrepancies in the signals.

This communication networks usually use the 5.8 and 5.9 GHz bandwidth for open communication as this makes the capabilities of broadcasting easier [1]. The latest advancements in the field are working on the safety of the traffic which are dependent on faster information exchanges if dangers are detected, this paves the way to the optimization of the shadowing effects and the fast fading effects which are induced due to constant motion of the vehicles, also the environmental conditions and surroundings in which the travel is as the surroundings tend to decrease the efficacy of the signals and can lead to information loss which must be reduced.

There are several ways of communication and information exchange in the system the VANET use not only the Wi-Fi but also the communication services such as 2.5G, 3G, LTE, 5G, Bluetooth, and more similar communication devices [2]. Each of this communication modes have their own advantages and disadvantages and have different effects on different scenarios as each of them have different capabilities which can vary according to the situation in which they are implemented for usage.

The VANET comes under the Intelligent Transport System which have also increasing interests and research in the present world. The integration of VANET with ITS was and always in study as there are many research that have proven that this can improve the drivability and road safeties which helps in decreasing the fatalities in the road by which the road users are benefited the most.

The wireless networks are the main communication devices that in which proper sensors must be attached to the transmitter and receivers which can improve the quality of information of the data transmitted. This ensures that there is less free space and path losses that occur in the model. The path losses in the model are calculated with the consideration of the frequency and the wavelength at which the signals travel between the transmitter and the receiver also considering the power, gain and the distance between the transmitter and the receiver.

Aim.

To develop a model that include the effects of fast-fading and evaluate the model for the accuracy to perform and experimentation for valuation of fast-fading considering various scenarios.

Tasks to reach aim of the project.

- To perform an analysis of the literature on the problems of the VANET network.
- Develop, based on existing experimental and theoretical work, a mathematical model that also evaluates the effect of fast fading.
- Perform experimental work and adjust the developed model based on them.
- Evaluate the accuracy of experiments by performing methodological measurements.
- Provide conclusions and recommendations.

1. Literature Survey

1.1. History of VANET

The history of VANETS dated to as early as 1922 when the first patent on Radio Warning systems for vehicles were published to facilitate the vehicle-to-vehicle communication process. There were several developments in the radio communications that were made in the military which were also developed for long- and short-range communication in the UAV using radio and other wired devices for distant operations in the years after. The radio warning system used in those days can be seen in Fig. 1 below.

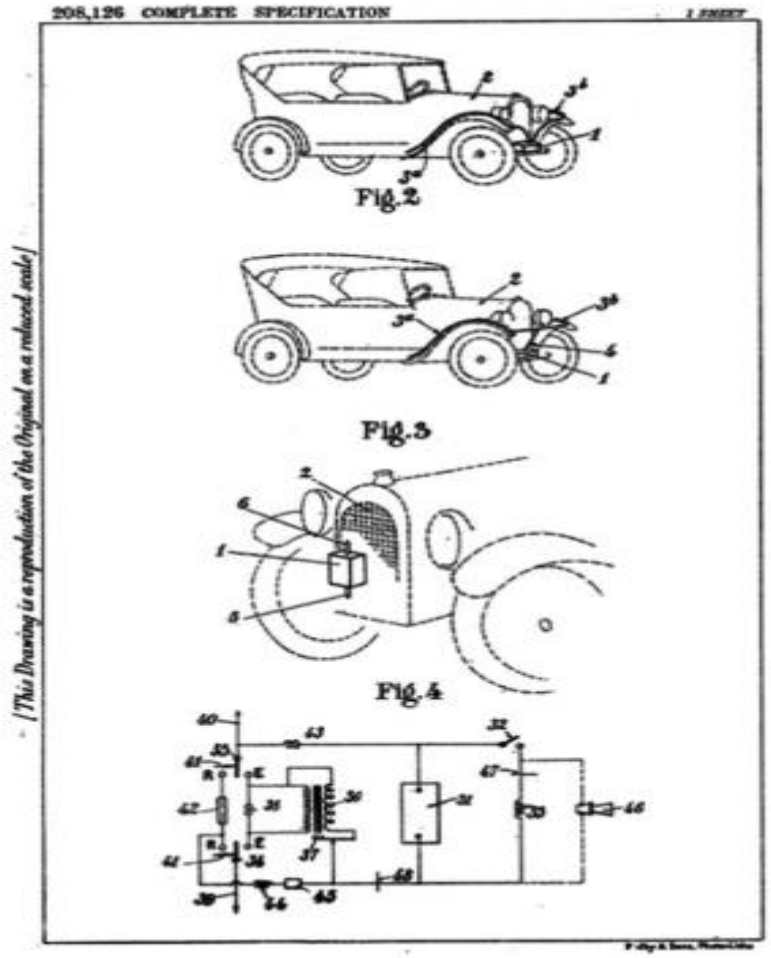

Fig. 1. Drawing from radio warning system for use in vehicles

However, after about half-a century the commercial and the passenger vehicles also had adopted radio sets in their vehicles which were used for hearing to local radio stations which were used to communicate about the weather and the surrounding traffic conditions over the air which were used. But all these communication channels were considered unidirectional and not bi-directional meaning they were only able to receive signals but were not able to transmit any data. Later till Radio Frequency Identification (RFID) were introduced for tolling stations that is when the effect of bi-directional communication was known. It was first with 2.45 GHz frequency in Europe which was later changed into 5.8 GHz also in the rest of the world and the USA operating with 915 MHz, with this Philips, who has invented the dedicated short-range communications (DSRC) which created a pathway for the Intelligent Vehicle-Highway systems. The vehicles now have various advanced technologies for communication and have Bluetooth connection for better connection [3].

1.2. Standards and Regulations

There are several standards and regulations that are created by various organizations which are the bodies that are creating the regulations and rules for the Intelligent Transport Systems (ITS) namely, International Standards Organization, IEEE, Society of Automotive Engineers, ETSI, International Telecommunication Union, and CEN are some of the major organizations.

Among administrative SDOs, the primary support on ITS standards is the International Standards Organization (ISO) Technical Committee (TC) 204 "Intelligent Transport Systems." ISO/TC 204, created in 1992,2 with its 18 working groups (WGs), is accountable for the global structure and structure characteristics of ITS, bringing into account the work of present worldwide regulation societies. ISO TC2 04 collaborates with the Comité Européen de Standardization (CEN) TC 278 ITS, 3 emerging mutually CEN/ISO standards.

CEN/ISO are operating on all levels and bodies in the ITS protocol stack with a international scope fulfilling the demands of all stakeholders (i.e., road users, city organisations, car manufacturers, cellular network operators). The configuration of the WGs is seen in Fig. 2.

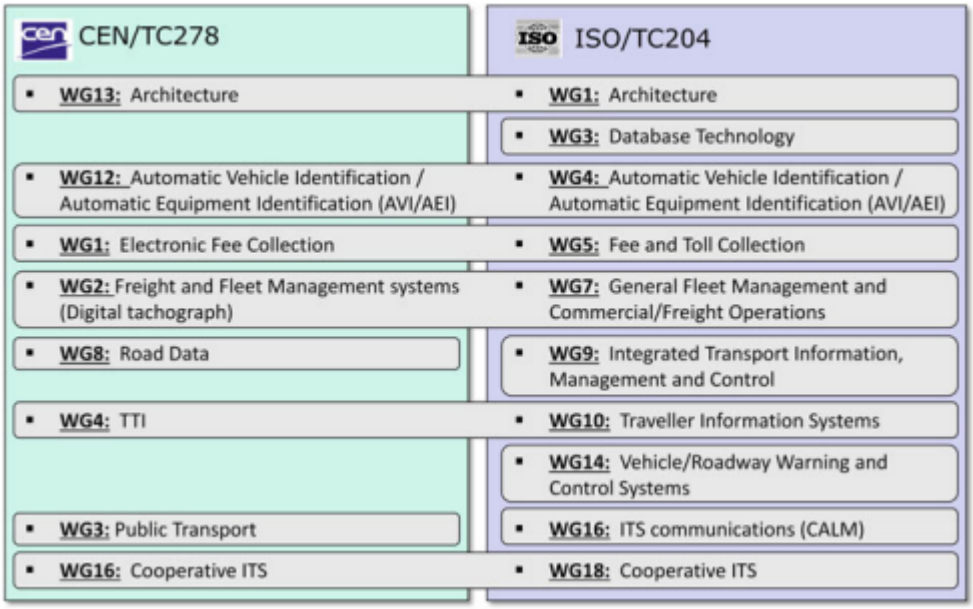

Fig. 2. Joint development of standards by CEN TC278 and ISO TC204 [4].

The International Telecommunication Union (ITU) lately just attempted to started conception of a unit for ITS. No standards are presented yet.

Amongst non-legislative SDO, as an enterprise of members of ISO TC204 WG16 "Wide Area Communications"—also known under the work designation of "Communications Access for Land Mobiles" (CALM), the European Telecommunications Standards Institute (ETSI) TC ITS was initiated in 2007 in direction to profit from quicker procedures in ETSI and the ETSI capability centre on testing. In tradition, ETSI followed a car-centric method centered on a single protocol stack for car-to-car and car-to-roadside communications with C-ITS applications for road safety and traffic efficiency.

Institute of Electrical and Electronics Engineers (IEEE) standards such as IEEE 802.11 are used for ITS, and IEEE 1609 WG5 advanced a set of standards under the work label "Wireless Access in

Vehicular Environment" (WAVE), which is an enhanced sub-system of ITS with a precise own architecture and a foremost focus on IEEE 802.11 access technology.

A additional corporation emerging standard-like terms is the Society of Automotive Engineers (SAE) in the USA with a emphasis on requirements of data dictionaries, also referred to as message sets. SAE collaborates with CEN, ETSI, and ISO.

In Japan, Association of Radio Industries and Businesses (ARIB), Japan's regulation institute, operates exploratory studies, investigation, and improvement on C-ITS. ARIB standards are already employed in large measures.

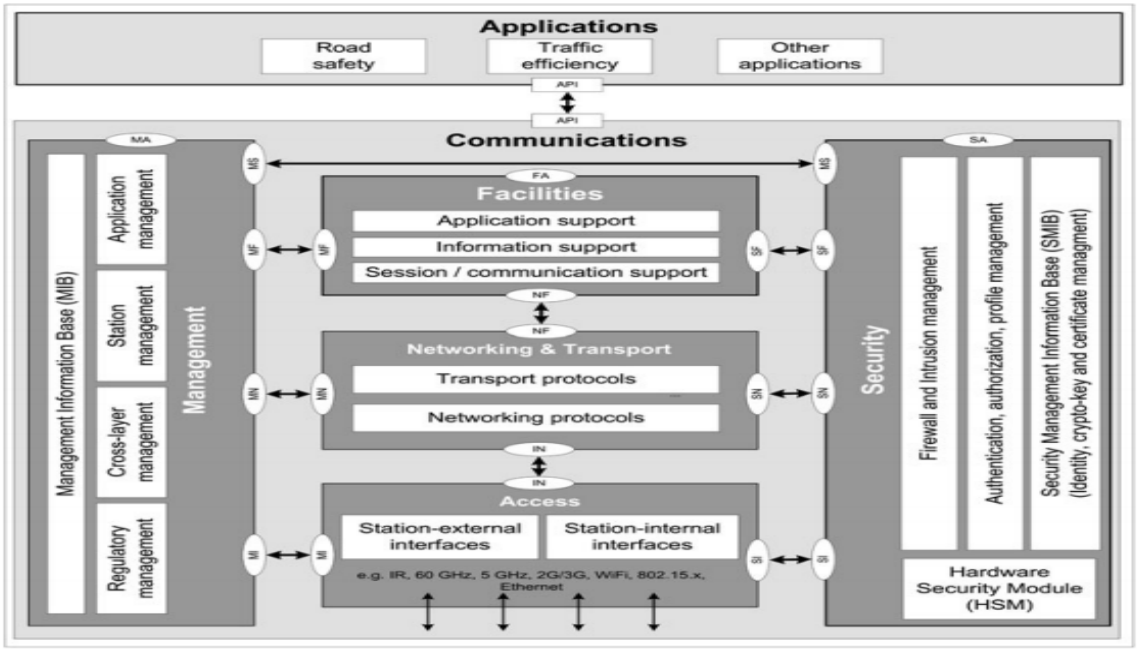

Fig. 3. ITS Station reference architecture [4].

There are different standards and harmonization that were discussed by Fischer which explains the factors that are considered for modelling and building of a network architecture which are important. The architecture of the ITS as per the guidelines given can be seen in Fig. 3 which shows the station reference architecture [4].

1.3. Fundamentals of VANET Communications

There are several important technical terms that are part of the VANET which are the building blocks for the technology. The terms and the factors that affect the VANET communication systems can now be discussed in detail.

Signal Attenuation is the diminishing strength of the signal during its transmission; this is usually related to the path loss and the receiver's loss. Fading is also a loss of signal, but this occurs due to the change in phase of the receiver as receiver wave travels in different travel path. Attenuation and fading are both different sides of the same coin where the loss in the signal is attained in different methods.

Antenna gain is the factor that is characterized by the quality of the signal transmitted and received. There are also other factors such as the interference as the name suggests when the signal travels between the transmitter and receiver the signal is blocked with some interference. Noise in the signal

is the variation or fluctuation that is received in the transmitted data. Sensitivity is the minimum input that is required to give an output to a signal. Coherence time is the duration in which the channel impulse response is considered not varying.

In fading there are different types of fading which occurs, and they are classified as fast and slow fading. In slow fading the coherence time is relatively large to the delay requirement. Slow fading is usually caused due to shadowing which is affected by some surrounding obstruction such as hill, buildings and other environmental hindrances that can block the signal and cause attenuation. Fast fading is phenomenon that occurs when the coherence time is relatively small to the delay requirements. This occurs when there is change in the phase of the receiving and the transmitting channels which changes when there is change in their distances, for example it can be the signal fading that occurs when two vehicles are travelling at different phases [5].

1.4. Models and Theories for Developments

There are different models that were investigated for the slow and fast fading analysis. One of the models which were used in majority for the development of the new model were Poryazov in which he has developed a model based on PSTN and GSM which were mathematically analysed, the model was simulated in real PSTN, the data were verified both mathematically and with experiments [6].

Later Poryazov et.al., also proposed some more tele traffic equations using the same model that was developed earlier which had been simplified to many parameters and can easily be calculated on other parameters which can improve the effects, that are on the model. The conceptual model of the telecommunication system and its environment and its environment in Fig. 4 as stated by the author can be seen below. [7].

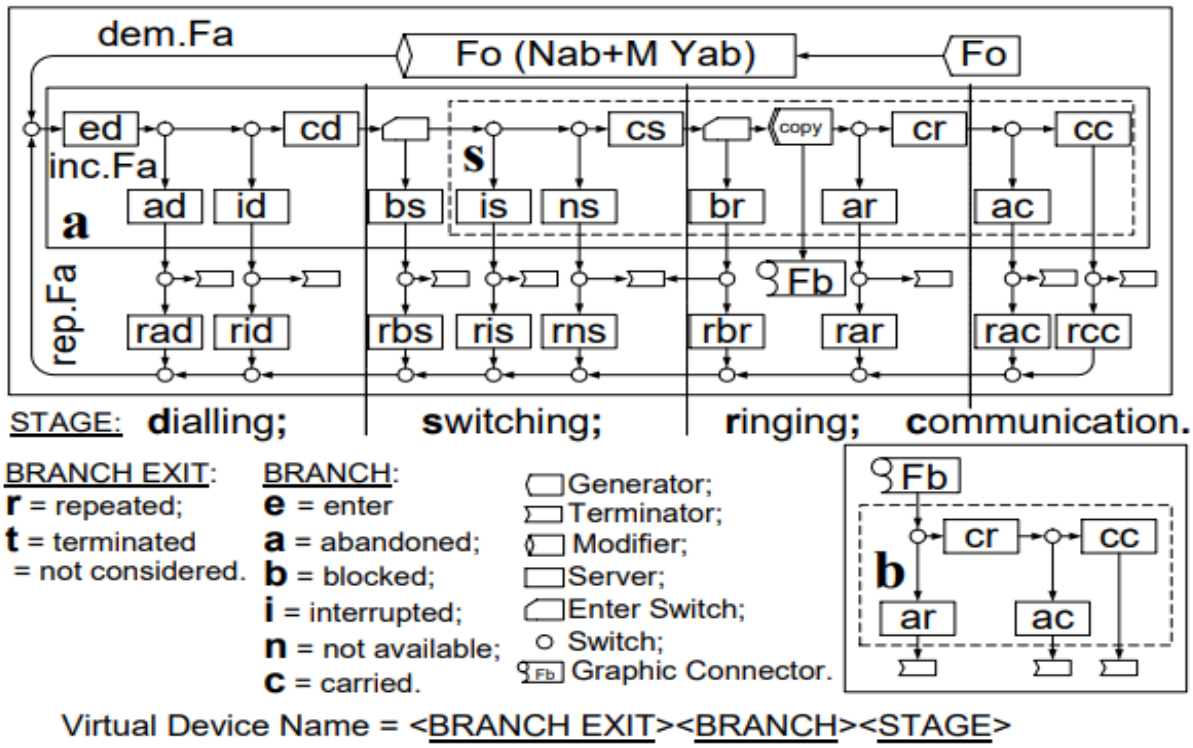

Fig. 4. Conceptual model of telecommunication system and its environment [7].

Matolok in his paper has discussed briefly about the V2V communication system, the channel modelling involved, and the various parameters and the roles played by it in the modelling of the V2V infrastructure, a potential channel classification model can be seen in Fig. 5. Path loss, delay spread, and Doppler spread is also addressed with which a potential channel classification for the communication system is in parking garages, inclined planes are also considered for the analysis and the results in the channel [8].

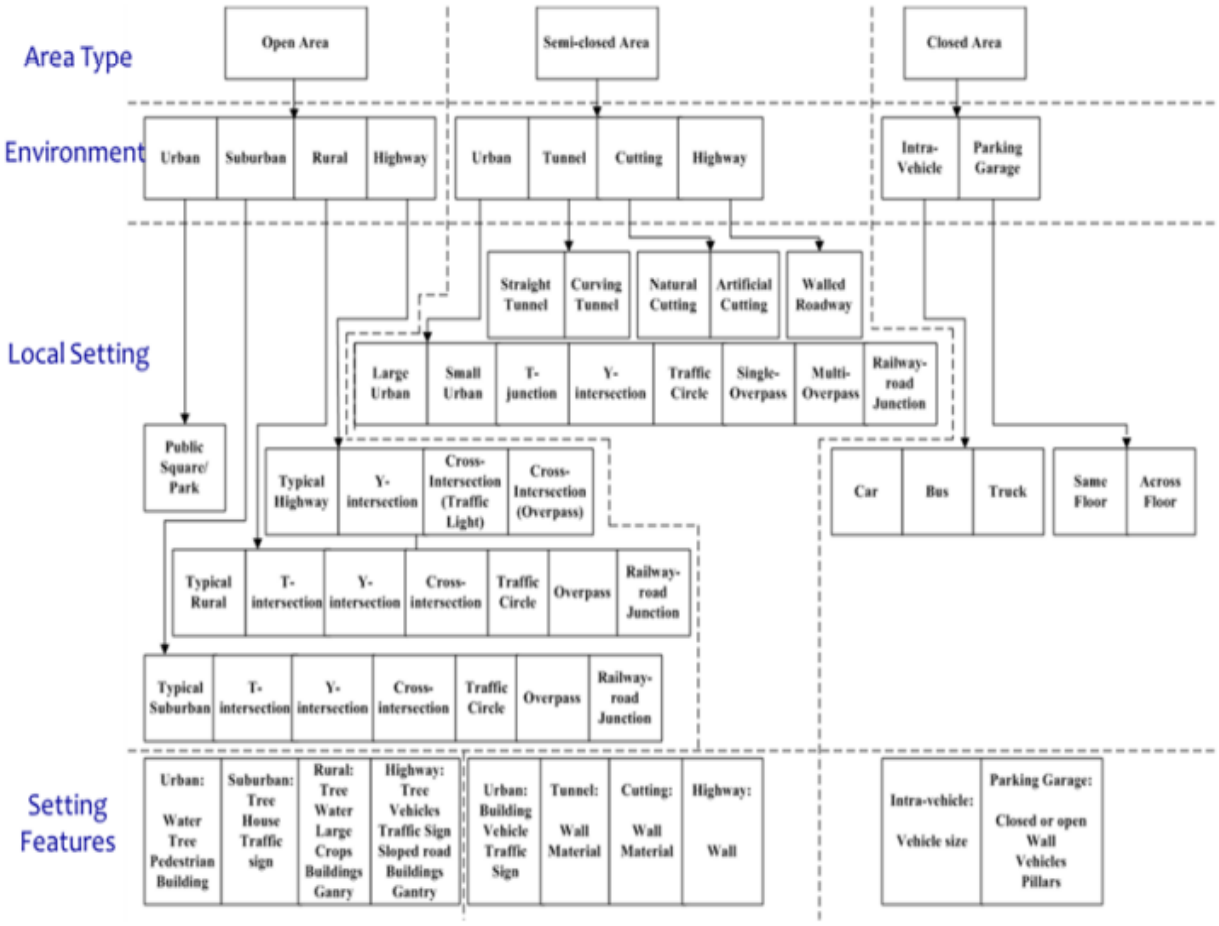

Fig. 5. Potential V2V channel classification scheme [8].

Demien et.al., in their paper have developed a design of shark fin shaped antenna for the automotive systems with a 5.9GHz antenna and various other communication sources such as LTE, GSM, DCS, etc., this showed different coupling cases which were used and challenges involved in the coupling of the different use cases in an confined space which paved way to the analysis of multiple LTE bands being tested by coupling 2*2 LTE-MIMO for better results. This suggests that the shape of the antenna also has effect on the signal transmission and has varying efficiency [9].

Alejandro Martínez et.al., have made an analysis for low-cost communication for implementation in the V2I application in which they have compared the different technologies namely, Wi-Fi, LoRa, ZigBee, Z-wave, Bluetooth, nRF24 with respect to the bandwidth their distance of operation, data rate, protocol, and the availability of network. Based on the considerations a decision tree was made for easier decision of the system to be used according to the cost of the technology which can be seen in Fig. 6 [10].

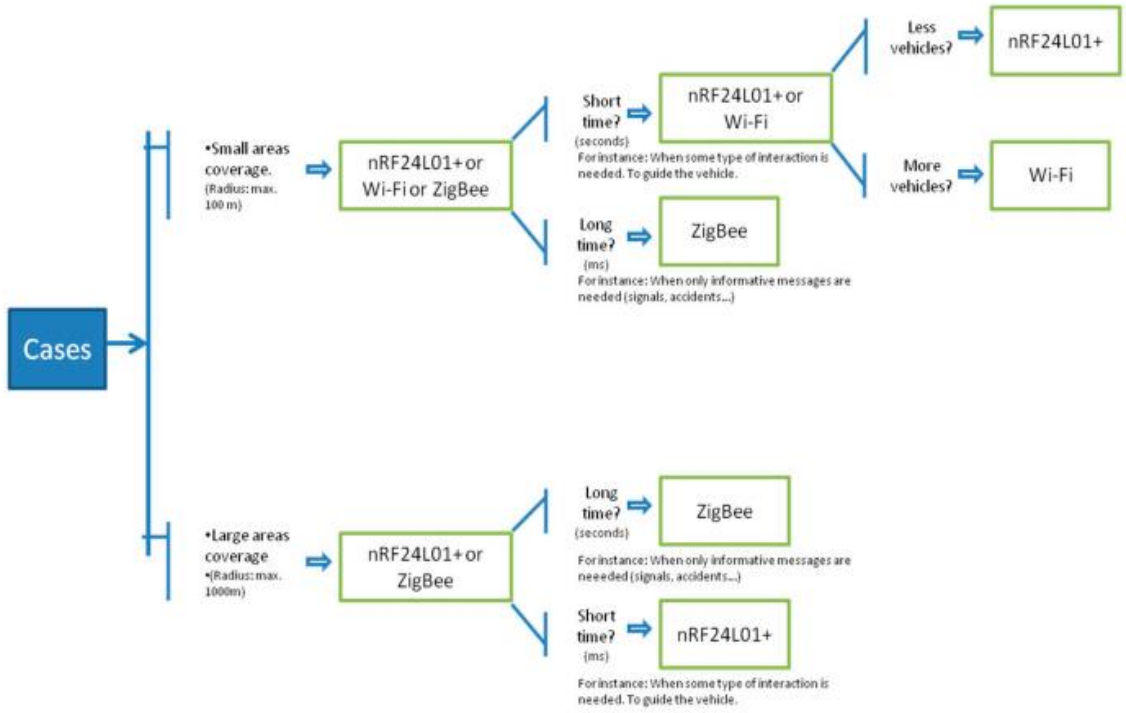

Fig. 6. Decision tree for the device [10].

Wenshuang Liang et.al., in his article has discussed briefly on the different architecture in the VANET's and their challenges and trends in which they are implemented. The security, routing, and the privacy of the VANET's which were the major research issues in the field and its application were analysed with different architecture. The V2V architecture can be seen in Fig. 8. The VANET system domain can be seen in Fig. 7 can be seen in the below picture in which the mobile domain consists of the vehicle and the mobile devices. Generic domain consists of the internet infrastructure and private infrastructure domains and the infrastructure domain consists of the roadside infrastructure and central infrastructure domains. These domains for the basic operation for the VANET [11].

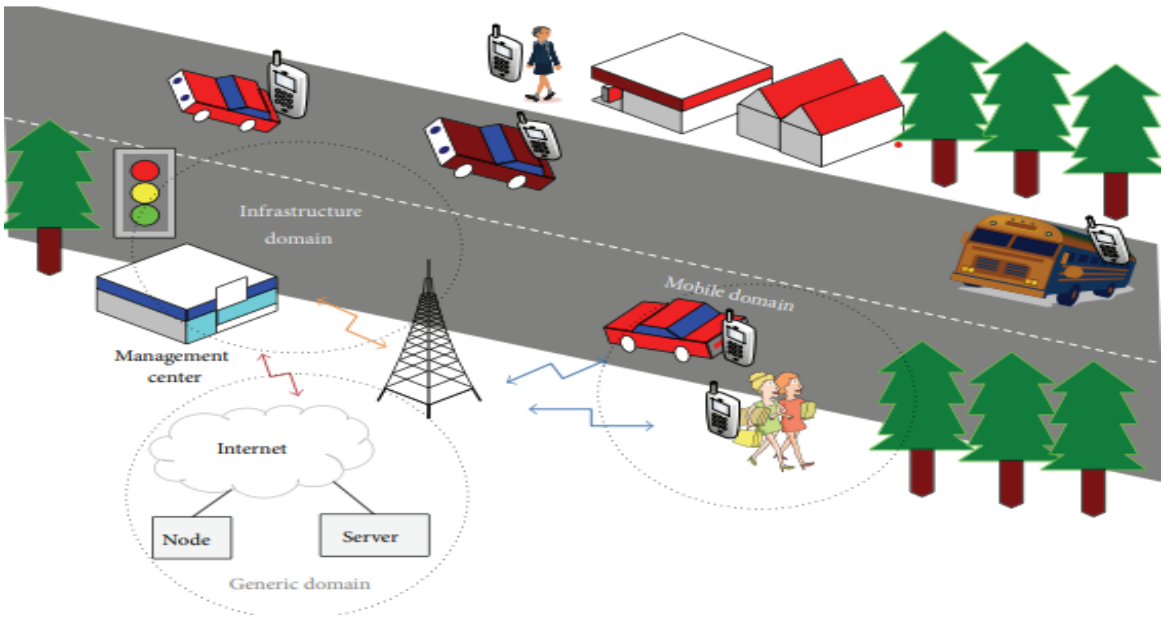

Fig. 7. VANET system domain [11].

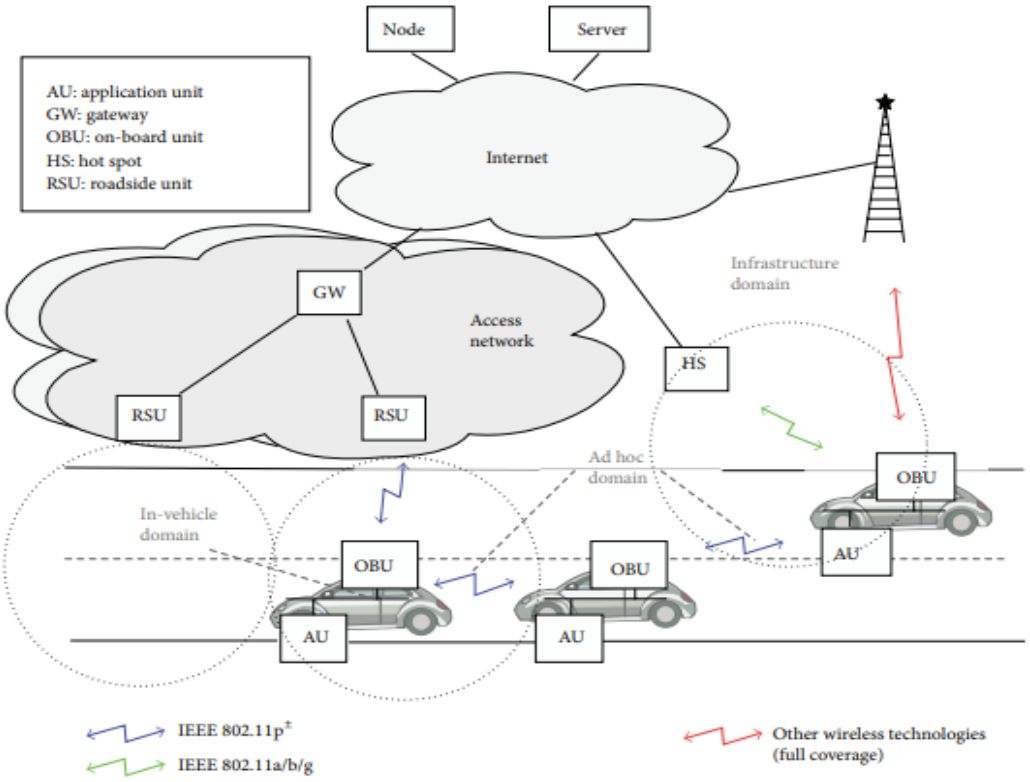

Fig. 8. V2V architecture [11].

Zaigham Mahmood in his article has discussed briefly on the connected vehicles in the Internet of Vehicles, in which the internet of thing of connected vehicles based on the VANET where the connected autonomous vehicles the various topologies and their architecture. The various protocols, handover and the efficacy of the connection is all analysed [12].

Akira Sakuraba et.al., has made a performance evaluation of vehicle to vehicle and vehicle to road communications on two wavelength cognitive wireless networks. According to this system the fundamental functions that this can perform whereby, observing the state of road surfaces by multiple sensors on the vehicles, ad analysis of these data from the output obtained. The results obtained show that the data can be attained even when there are no such communication technologies such as 3g or LTE is available and has been evaluated to perform the best with transmission of good results [13].

Satoshi TAKAHASHI et.al., in her article has analysed the distance dependency of path loss in inter-vehicle communication, the millimetre-wave path loss between two cars were measured to determine the applicable distance for inter-vehicle communication. The measurements were done on the highway considering the parameters such as the driver giving way to pass-by etc which are relatable to the real-life scenario. The path loss was observed to be high in crowded highways [14].

J. S. C. Turner et.al., has discussed on the various vehicle channel models, the large -scale path loss where the two-ray model and the log-scale models are reviewed, also the small-scale fading models of Rican, Rayleigh, Weibull, Nakagami have a brief introduction as these play a major role. XBee technology were used for the transmission and receiver the attenuation, first Fresnel zone etc were all considered and concluded that the obstruction, and several other parameters such as ground surface and their effect on the path loss were analysed and accounted [15].

Nabeel Akhtar et.al., has analysed the temporal and spatial advancements of VANET using modelling with SUMO where a macroscopic mode is used. The cumulative distribution function is analysed with respect to factors such as link duration, nodes, clusters formed, etc. The validation of the model was made based on the data that were obtained from the real scenario in highways [16].

Imene Trigui et.al., had evaluated the performance of downlink of cellular networks when fading occurs were evaluated. Various proof for the evaluation of different parameters and Rayleigh, Rican, fast and slow fading were analysed, and the performance were all considered and concluded [17].

Boban. M in the doctoral thesis published has made an efficiency analysis for channel modelling of vehicular networks. The impact of vehicular obstruction, the impact of static obstructions such as buildings, surrounding environments were experimented and the performance characteristics of different vertical displacement antenna were examined in the study. The key contributions were the evaluation of the efficiency of an inter-vehicle communication model, tall vehicle relaying techniques, geometry based computational efficiency of the model were all the factors that contributed to the research [18].

Taimoor Abbas et.al., had developed a shadow fading model for vehicle-vehicle network simulation was performed where a model was developed to measure the shadow fading parameters in the case of both LOS and NLOS, the transmitter and receiver were set up in two different vehicles and were tested in both urban and highway environment where the model seems to have shown good results of the separation between LOS, OLOS, NLOS are visualised with simulations which is seen in Fig. 9. The dual slope path loss model with respect to the distance is given as, [19].

$$PL(d) = \begin{cases} PL_0 + 10n_1 \log_{10}\left(\frac{d}{d_0}\right) + X_\sigma, & \text{if } d_0 \le d \le d_b \\ PL_0 + 10n_1 \log_{10}\left(\frac{d_b}{d_0}\right) + & \text{if } d > d_b \\ 10n_2 \log_{10}\left(\frac{d}{d_b}\right) + X_\sigma \end{cases} . \quad (1)$$

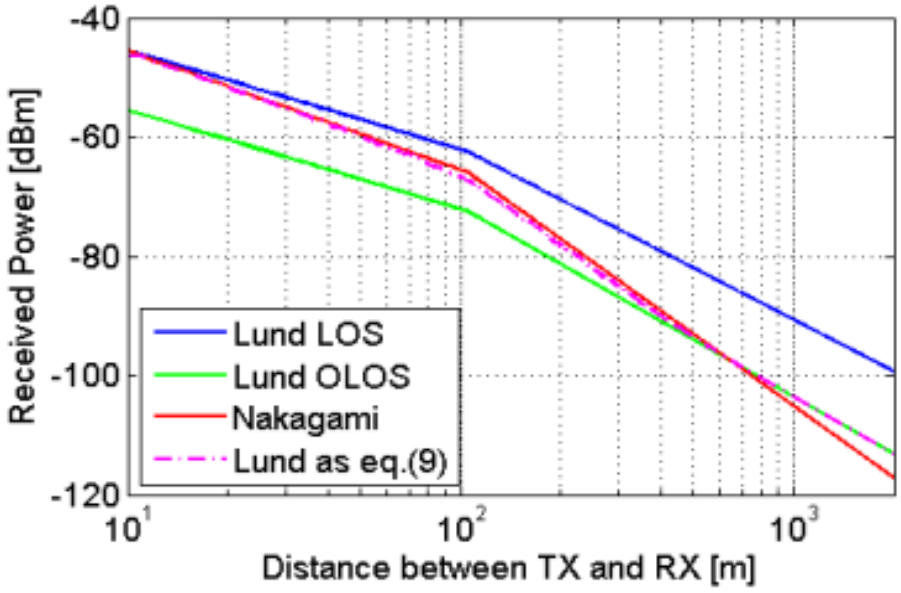

Fig. 9. Comparison of received power in various LOS models [19].

Khalid Abdel Hafeez et.al., in his findings has evaluated and simulated different models in NS-2 and MATLAB in which they have concluded that it is difficult to come to a conclusion with the simulation results for the implementation of a model but the Ricean distribution has shown better results in the highway scenario which can be recommended however, it is seen that the appropriate model choice can be accomplished only when tested in real-life scenario [20].

V.Lavanya et.al., had modelled fast fading channel for wireless networks in which the variations caused that lead to Rayleigh and shadow fading effects are analysed with theoretical, CDF, PDF are obtained and analysed with Rayleigh distribution and log-normal distributions are obtained which leads the way to the proper mitigation of the signals [21].

Julio Arauz et.al., has described the influence of discrete Rayleigh fading channelling model in which the validation was done by information theory analysis and stochastic validations for FSMC. The hidden Markov model (HMM) characteristics are analysed for which have better flexibility exists. It concludes with the advantages and disadvantages of the models [22].

Francisco J. et.al., had assessed the impact of radio propagation on application to VANET using real maps in which the map visibility schemes, RAV attenuation and visibility schemes are evaluated by simulation using different parameters. This resulted in the choice of using RAV in which the communication distance between the vehicles have increased from 250 m to 400 m using the same bandwidth but with 802.11a protocol and have better notification time which gives more accurate results. The below Fig. 10 shows how the algorithm of LOS works based on which the model was developed and compared with various other schemes.

$$\begin{aligned} \alpha'(i,j) = & \left| \operatorname{atan} 2\left(\left|y_i^2 - y_i^1\right|, \left|x_i^2 - x_i^1\right|\right)\right. \\ & \left. -\operatorname{atan} 2\left(\left|y_j^2 - y_j^1\right|, \left|x_j^2 - x_j^1\right|\right) \right| \\ \alpha(i,j) = & \, min(\alpha'(i,j), 360 - \alpha'(i,j)) < th_a \end{aligned} \quad . \tag{2}$$

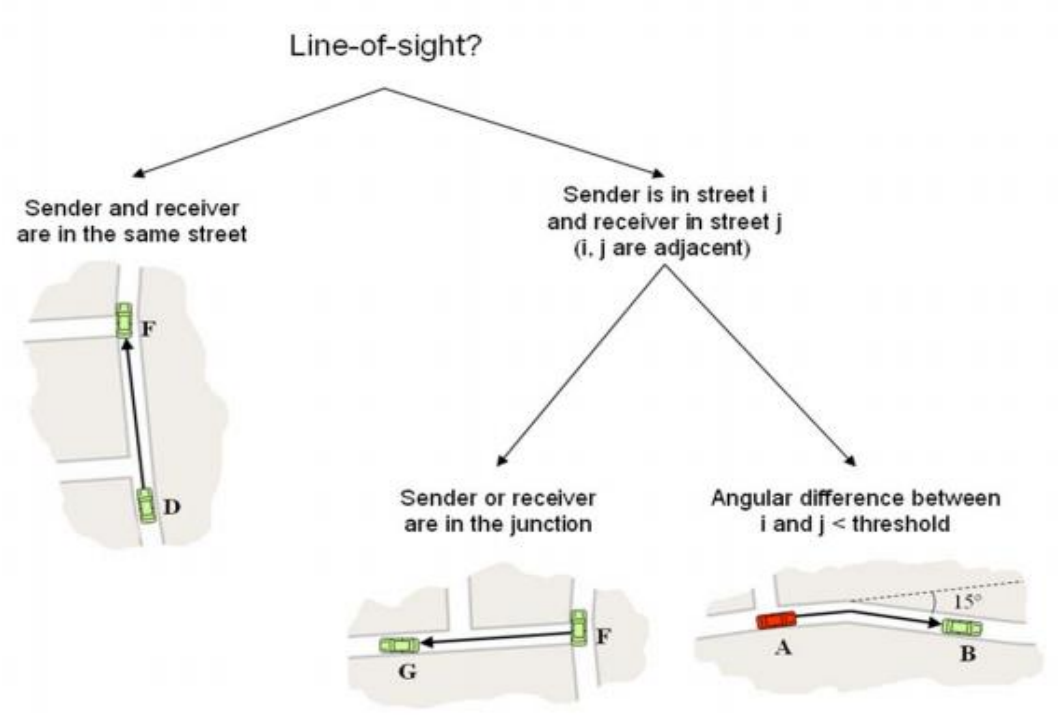

Fig. 10. RAV algorithm [23].

There are two different schemes that are considered and adopted in the developed model in which the attenuation scheme if implemented in the simulation software NS-2 it is observed that there was considerable amount of packet loss error when calculated as the software tends to not receive the signal if there is collision this has made the authors to develop a probability distribution function with a fourth degree polynomial for packet error rate with Euclidian distanced between the vehicles using regression coefficients. Fig. 11 shows the RAV visibility scheme in the software and Fig. 12 plots the comparison of the different attenuation schemes [23].

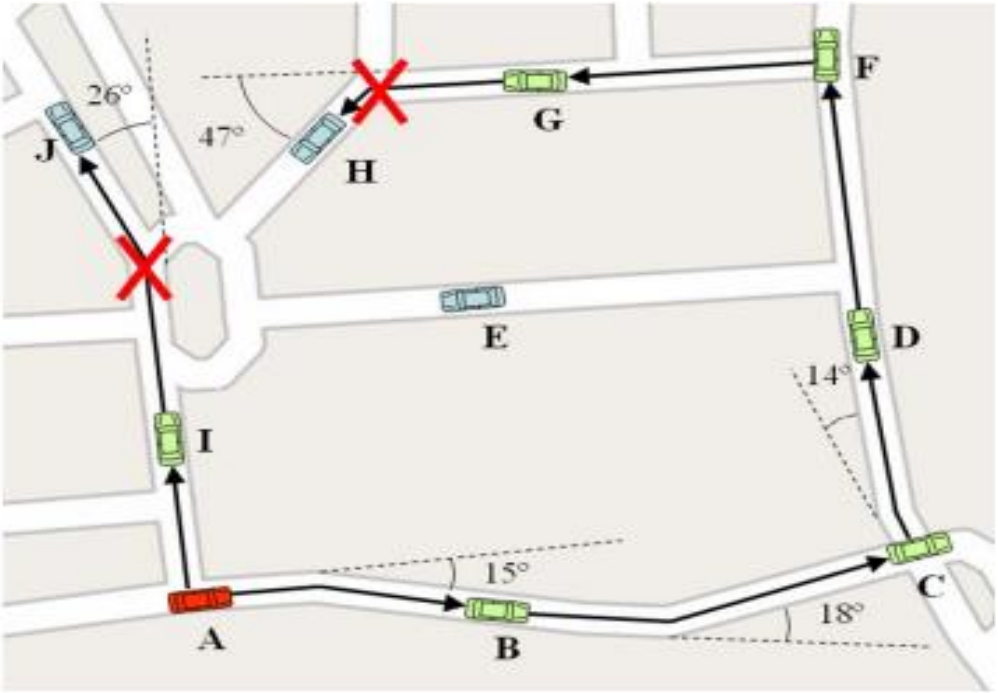

Fig. 11. Example scenario of the RAV visibility scheme in the simulation software [23].

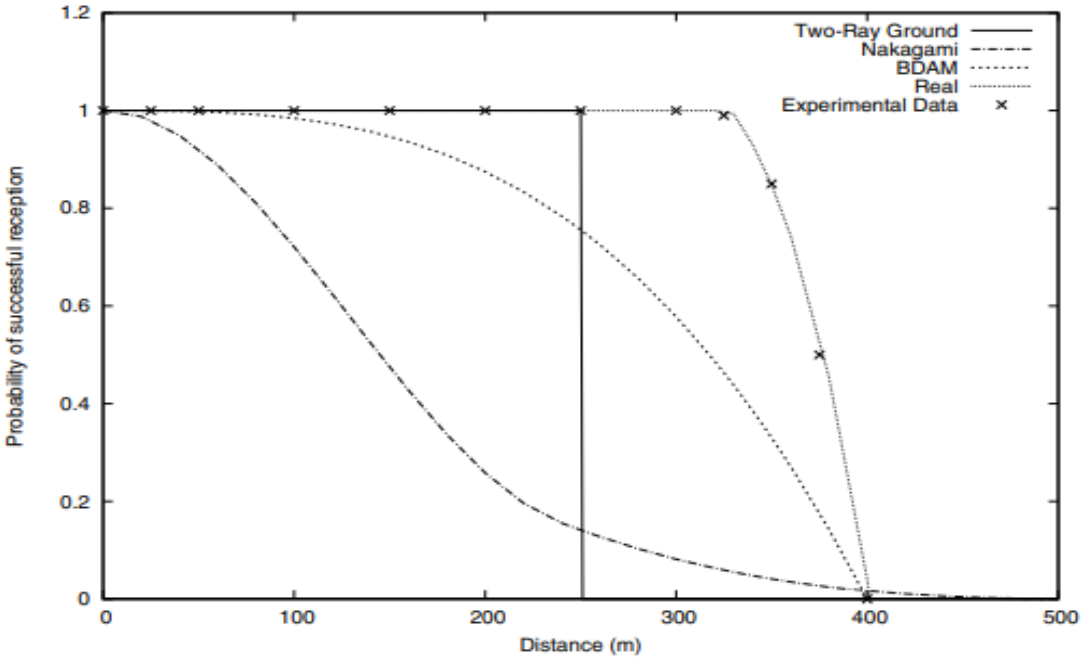

Fig. 12. Comparisons of different attenuation schemes [23].

Al-Absi, M. A. et.al., in his paper had proposed the CHR model that is obstacle based the path loss and shadowing in the city, highway and rural areas are the channel parameters that are analysed and simulated, and the results of collision achieved, transmission performance, throughput of the traffic, collision performance at different environments are the results that are obtained. The flow diagram of the model is seen in Fig. 13.

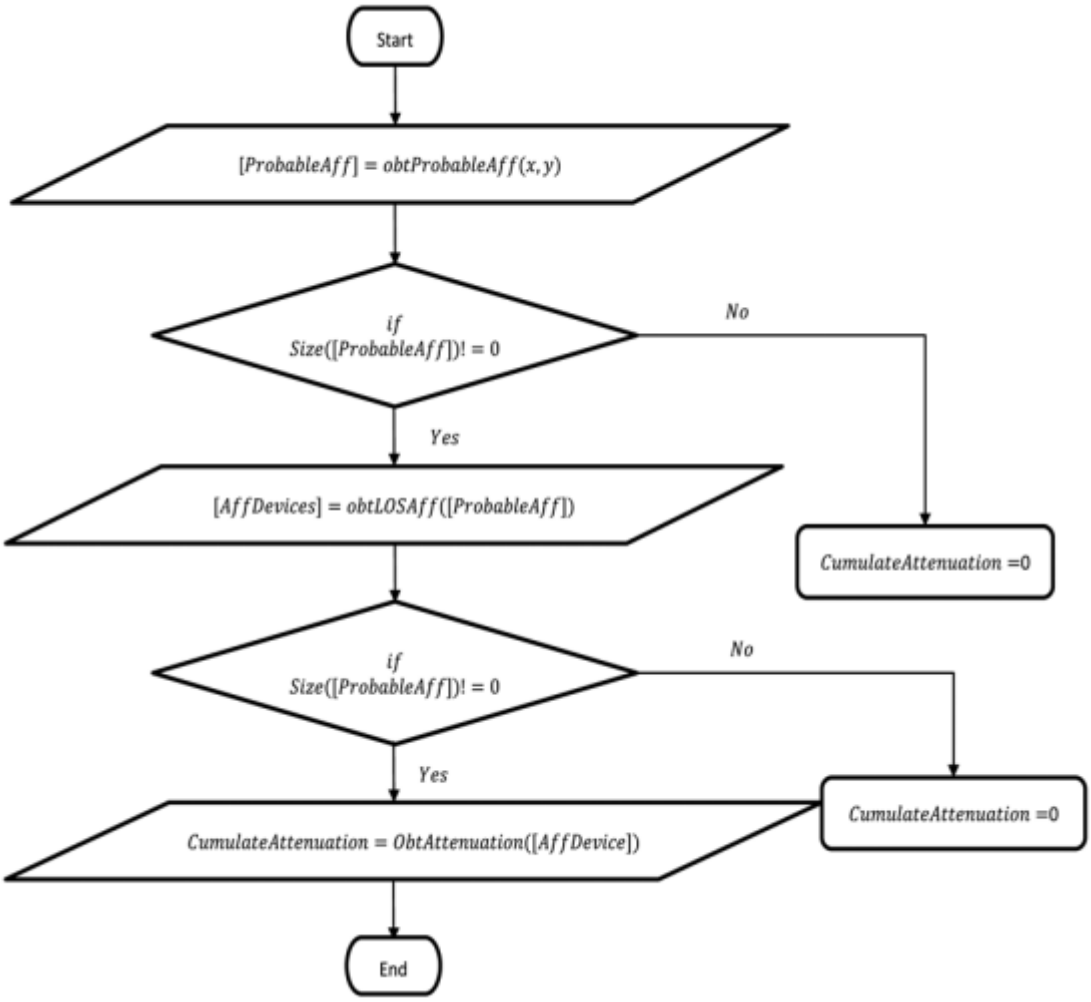

Fig. 13. Flow diagram of the obstacle proposed based on CHR model [24].

The model development goes as follows and the equation used with respect to the speed and the density of vehicle is calculated.

$$\mathcal{M} = lu\ . \tag{3}$$

The Fresnel ellipsoid is formed by the VANET devices is obtained using the below equation,

$$z = \left(z_y - z_x\right)\frac{r_{aff}}{r} + z_x - 0.6s_k + z_t\ ; \tag{4}$$

where z_t is the device antenna altitude, r is the distance among transmitting and receiving devices, r_{aff} represents the distance between obstacle and source device, z_x and z_y are the altitude parameters of source and receiving device of x and y, respectively, r_{aff} represents the distance between obstacle and source device, and s_k is the range to obtain primary Fresnel zone ellipsoid is represented as,

$$s_k = \sqrt{\frac{W r_{aff}(r - r_{aff})}{r}} \; ; \tag{5}$$

where *W* represents the wavelength. Finding the altitude of all probable obstacle devices is prior to transmission as a key factor and considers that the device will obstruct LOS among source and receiving devices if *z* is higher than its altitude. Thus, the likelihood of LOS among device *x* and *y* is computed as follows,

$$L(\text{LOS} \mid z_x, z_y) = 1 - Q\left(\frac{z - \varphi_z}{\omega_z}\right). \tag{6}$$

With this likelihood the article proposed model of CHR with obstacle-based radio propagation model, the collision, efficiency of throughput and performance of transmission in distributed slotted MAC. There are various problems with the MAC as its design requires various changes in their efficiency so adaptive MAC is also proposed for the future works [24].

Van Eenennaam, E. M. had in general explained about the models used in VANET simulations are surveyed and their influence on how they affect the path loss and shadowing exponents are tabulated and visualised. Due to varying environmental conditions the VANET simulations cannot be accepted in a realistic scenario, so it is recommended that the deterministic model be done stochastically [25].

Qureshi, M. A. et.al., proposed a model with a lightweight radio propagation model for communication in the tunnels in which they measured and validated values for different stationary and dynamic scenarios in which cases the received signal strengths were calculated and compared with the distance between the transmitter and receiver and the distance between the communicating vehicles. It is seen that in the proposed model the path loss is less when compared to other models, with high packet delivery ratio.

The model is based on the general log-normal path loss with respect to the distance between the communicating nodes, *k* is the constant of proportionality for road tunnels.

$$PL_M[dB] = k \log_{10}(d). \tag{7}$$

$$k = r + \frac{w}{h\lambda} \; . \tag{8}$$

Where, *w* is the width of the tunnel, λ is the wavelength of the signal, *h* is the height of the tunnel and *r* is the difference in height and width of the tunnel.

$$PL_{AM}[dB] = 6.9 + 20 \log_{10}\left[\sqrt{(v - 0.1)^2 + 1} + v - 0.1\right]. \tag{9}$$

Where, $v = \sqrt{2}\,\frac{H}{rf}$, H is the difference in height of radio obstacle and the height of straight line connecting the communicating vehicle. This part brings in also the Fresnel zone of the vehicle which will be considered with which the model is obtained as shown in the below equation, where *F* is the probability of large moving obstacles interrupting the line-of-sight between the vehicles.

$$PL[dB] = PL_M[dB] + F(PL_A[dB]). \tag{10}$$

The comparison of the measured and proposed model is seen in the above model with the path loos being constant without much fading is observed also the model is compared with other existing models which is seen in Fig. 14 which depicts that there is less path loss at higher distances in the

proposed radio propagation model and Fig. *15* shows the comparison of the path loss prediction in various models [26].

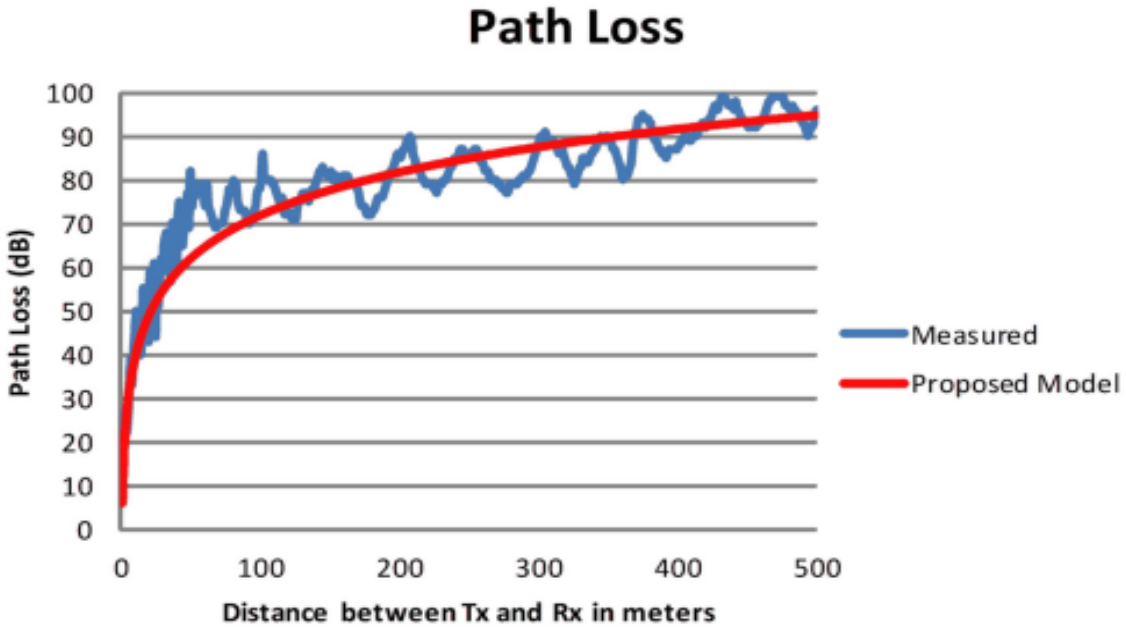

Fig. 14. Comparison of Pathloss in measured and proposed model [26].

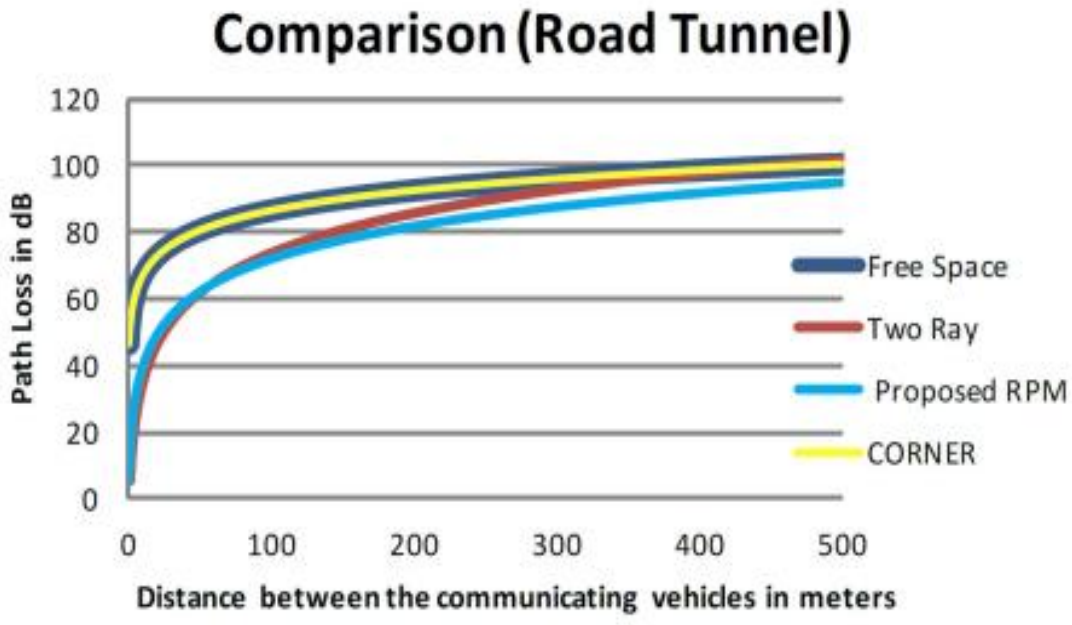

Fig. 15. Comparison of predicted pathloss [26].

Chandrasekharamenon and Anchare V had briefly discussed about various models namely Rayleigh, Rician and Weibull with their impact on the parameters such as path loss exponent, shadow fading, and fading factors were analysed. Assuming vehicle speed to be random with truncated Gaussian distribution the vehicle speed distribution statistics were presented which were validated by comparing the simulation results with theoretical models [27].

Ehsan Mostajeran et.al., has developed a model for urban grid environment, using JiST/ SWANS simulator a realistic environment was designed with which the path loss model was applied, and the results were obtained the path loss were also calculated for both LOS and NLOS type of transmission for which the comparisons of the performance were evaluated [28].

Mukunthan, A. et.al., has analysed and evaluated a corner propagation model in urban environment. In NLOS situations the Rayleigh fading was applied and Rician for LOS scenario. The comparison and the results evaluated show that there is a significant drop in the packet delivery due to fading and tends to increase this nature as the density increases [29].

1.5. Problem Statement

The VANET communication systems are upcoming technology and various factors that affect its efficiency are being in research for quite long now and there are several research in this area as many countries are planning to implement ITS and smart city project in which VANET is an essential part. There are many research that solve the gain, power, signal attenuation, privacy issues that are addressed but on the other hand the losses in the signal due to shadow fading and fast fading are less considered. A recommendation of a new model in which both the fast fading and shadowing of the signal is being developed in this research were the data are taken from various source which used for the evaluation of the model developed.

1.6. Novelty of the work

1. The intent of this work is to develop a model that includes the fast-fading effects in the VANET's.
2. The theoretical and the experimental analysis of the model is done with an accuracy score of 96.95%.
3. The log-normal path loss model is chosen as the basis for the development of the model and the experimentation to evaluate for fast fading is performed after the evaluation of accuracy of the model.
4. It has been observed that at distances up to 50 m, both slow and fast fading occur, while at distances greater than 50 m, slow fading predominates.

2. Methodology

2.1. Fading

In wireless propagation systems the fading is the loss of the signal that occurs due to various factors. There are various types of fading which is classified according to the type of loss that occurs which are discussed in detail below.

The main classification of fading is large-scale fading and small-scale fading, which are classified further classified based on the attenuation.

Large-scale fading is the attenuation of the signal due to obstruction that are between the transmitter and receiver and also the signal loss when transmitted long distance. This type of fading is further classified as path loss and shadowing.

Path loss is the signal attenuation that occurs due to the long-distance transmission. In general, wireless propagation signals tend to disperse in space as the distance is increased so the energy in the signal per unit area that is being transmitted tends to lose as the distance increases. This loss is attended by increasing the area of the receiver so that the spread can be captured.

Shadowing is the attenuation that occurs when the signal travels through obstructions this occurs due to the tendency of EM waves which travel through all the obstruction due to which it can lose some data on propagation. This loss is usually attended by LOS propagation in which the transmission occurs in Line of sight.

Small-scale fading is also called as Rayleigh fading in which attenuation occurs in small-distance and also including the measure of time. This is an important factor as it tends to decrease the efficiency of the data and tends to give error in the signal carried if not attended.

Fast fading occurs due to the movements that are observed in the transmitter and receiver in general in the case of VANET in between moving vehicles. Doppler spread is the main cause of this fading with Doppler bandwidth comparatively greater than signal bandwidth with faster channel variations, this causes linear distortions which is called Inter Symbol Interference (ISI) which is treated by incorporating adaptive equalizer.

Slow fading occurs due to the shadowing effect that is on interactions with the surrounding environment such as building and other obstructions which has effect on LOS. This affects the signal-noise ratio (SNR) which can be rectified reducing the error and designing the receiver geometrically.

Multipath fading occurs when signal is received and attenuated from various paths this is usually possible in multi-path propagation and it affects all frequencies which also causes phase distortions and ISI this occurs in two ways namely, flat fading in which all frequency components gets affected equally which causes amplitude to fluctuate. Selective fading is when a selective frequency of the signal is attenuated and disturbed this can be overcome by orthogonal frequency division multiplexing (OFDM) which would prevent data loss.

2.2. Scenarios for Experimentations.

2.2.1. Scenario 1: Cars one behind another.

In this the cars are parked behind one another in a parking lot as seen in Fig. 16 and the reading of the signal power is taken from 50 m and 70 m. The mean of the obtained signal is calculated to obtain the free space losses that occur while the hotspot is kept outside the car and then the same readings are also taken from placing the car inside the car. In the same scenario the values for the car while moving towards a point is taken from 70 m which is covered with a speed of 20 km/h is taken with which the fast-fading and shadow fading effects are also taken into account.

Fig. 16. Scenario 1

2.2.2. Scenario 2: Cars against one another.

As shown in the Fig. *17* the cars face each other in this scenario and the readings are taken from 50 m and 70 m length with InSSIDer. The average value of the received signal is calculated by taking 10 readings each from each car the hotspot is placed inside and outside the car to get the clear picture of how the free space losses affect the signal strength that is received in this case. This scenario is also performed while moving the cars with the same setup as mentioned above and the output of the received power is noted for further calculations.

Fig. 17. Scenario 2

2.2.3. Scenario 3: Cars in parallel

In Fig. *18* the cars are parked in parallel in the parking lot at distances 50 m and 70 m length the power received is noted and while in movement towards a point. The received signals in both the cases are tabulated to find the fast and shadow fading.

Fig. 18. Scenario 3

2.3. Experiments accuracy

The model evaluation and the accuracy are got from the readings that were taken in the above-mentioned scenarios and the accuracy of the signal received was calculated for two different transmission power of 20 dBm and 10 dBm. Two transmission powers are considered in order to check the accuracy and to point down to one value as the transmission power calculations are not easier to calculate. For this purpose, the received signal was measured in different distance in free space with which the path losses are calculated, and the transmission power can be obtained.

The transmitted power is calculated as shown below,

$$P_R = P_T + FSL + X_\sigma + X_F \, . \tag{11}$$

From this the transmitted power from the device is found to be 10 dBm as the transmitted power, when calculated matched the value of power received.

The mean variance, absolute error, relative error with the Gaussian distribution its skewness and the kurtosis are calculated for the received power in both open areas and when the device is placed inside the car. The theoretical and the calculated values for a scenario are compared and the accuracy of the values obtained is verified, which can be seen in the figures below.

Table 1. Variance and Gaussian for accuracy in open area with experimental values and relative error.

	Frequency 2.45 GHz	P_{Tx}=10 dBm							
d (m)	P_R (dBm)	PL(dBm)	Mean (dBm)	σ^2 (variance)	σ	ΔPL (absolute error)	ΔPL mean	($\Delta PL/PL$)* 100% relative error	Gaussian
50	-67	77	79.4	9.31	3.05	2.4	2.38	3.12	0.10
50	-71	81	79.4		3.05	1.6		1.98	0.11
50	-74	84	79.4		3.05	4.6		5.48	0.04
50	-71	81	79.4		3.05	1.6		1.98	0.11
50	-67	77	79.4		3.05	2.4		3.12	0.10
50	-66	76	79.4		3.05	3.4		4.47	0.07
50	-69	79	79.4		3.05	0.4		0.51	0.13
50	-69	79	79.4		3.05	0.4		0.51	0.13
50	-69	79	79.4		3.05	0.4		0.51	0.13
50	-70	80	79.4		3.05	0.6		0.75	0.13
50	-65	75	79.4		3.05	4.4		5.87	0.05
50	-69	79	79.4		3.05	0.4		0.51	0.13
50	-66	76	79.4		3.05	3.4		4.47	0.07
50	-68	78	79.4		3.05	1.4		1.79	0.12
50	-73	83	79.4		3.05	3.6		4.34	0.07
50	-71	81	79.4		3.05	1.6		1.98	0.11
50	-72	82	79.4		3.05	2.6		3.17	0.09
50	-77	87	79.4		3.05	7.6		8.74	0.01
50	-66	76	79.4		3.05	3.4		4.47	0.07
50	-68	78	79.4		3.05	1.4		1.79	0.12

Table 2. Theoretical values for the variance and Gaussian.

x	μ	σ^2	σ	Gaussian, d = 50 m
70	79.5	16.45	2.9	0.0006
71	79.5	16.45	2.9	0.0019
72	79.5	16.45	2.9	0.0049
73	79.5	16.45	2.9	0.0112
74	79.5	16.45	2.9	0.0228
75	79.5	16.45	2.9	0.0413
76	79.5	16.45	2.9	0.0664
77	79.5	16.45	2.9	0.0949
78	79.5	16.45	2.9	0.1203
79	79.5	16.45	2.9	0.1355
80	79.5	16.45	2.9	0.1355
81	79.5	16.45	2.9	0.1203
82	79.5	16.45	2.9	0.0949
83	79.5	16.45	2.9	0.0664
84	79.5	16.45	2.9	0.0413

85	79.5	16.45	2.9	0.0228
86	79.5	16.45	2.9	0.0112
87	79.5	16.45	2.9	0.0049
88	79.5	16.45	2.9	0.0019
89	79.5	16.45	2.9	0.0006
90	79.5	16.45	2.9	0.0002

In Fig. 19 it is seen that the experimental values of the normal distribution of the path loss, the mean of path loss and the standard deviation is compared with the path loss of the experimental and the theoretical values are compared which shows that the models accuracy ranging between 95-99% in open area.

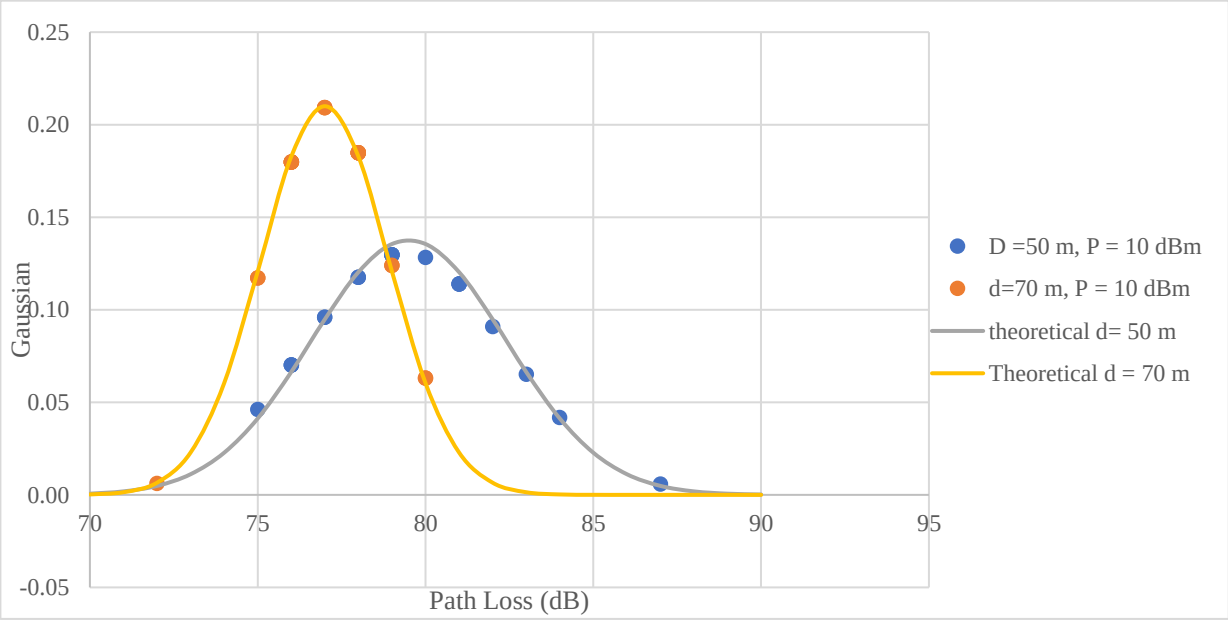

Fig. 19. Accuracy in open area

Table 3. Accuracy calculation when hotspot is inside the car with experimental values.

Frequency 2,45 GHz	P_{TX}=10 dBm								
car 1									
d (m)	*PR* (dBm)	*PL* dBm	Mean dBm	σ^2 (variance)	σ	*ΔPL* (absolute error)	*ΔPL* mean	(*ΔPL/PL*)* 100% relative error	Gaussian
70	-72	92	89.5	19.166	4.37	2.5	3.9	2.72	0.07742
70	-75	95	89.5		4.37	5.5		5.79	0.04139
70	-67	87	89.5		4.37	2.5		2.87	0.07742
70	-72	92	89.5		4.37	2.5		2.72	0.07742
70	-66	86	89.5		4.37	3.5		4.07	0.06620
70	-72	92	89.5		4.37	2.5		2.72	0.07742
70	-65	85	89.5		4.37	4.5		5.29	0.05373
70	-66	86	89.5		4.37	3.5		4.07	0.06620
70	-76	96	89.5		4.37	6.5		6.77	0.03027
70	-64	84	89.5		4.37	5.5		6.55	0.04139

Table 4. Accuracy calculation with theoretical values.

x	μ	σ	Gaussian, d = 70 m
80	92.5	5.3	0.005
81	92.5	5.3	0.007
82	92.5	5.3	0.011
83	92.5	5.3	0.015
84	92.5	5.3	0.021
85	92.5	5.3	0.028
86	92.5	5.3	0.035
87	92.5	5.3	0.044
88	92.5	5.3	0.052
89	92.5	5.3	0.061
90	92.5	5.3	0.067
91	92.5	5.3	0.072
92	92.5	5.3	0.075
93	92.5	5.3	0.075
94	92.5	5.3	0.072
95	92.5	5.3	0.067
96	92.5	5.3	0.061
97	92.5	5.3	0.052
98	92.5	5.3	0.044
99	92.5	5.3	0.035
100	92.5	5.3	0.028

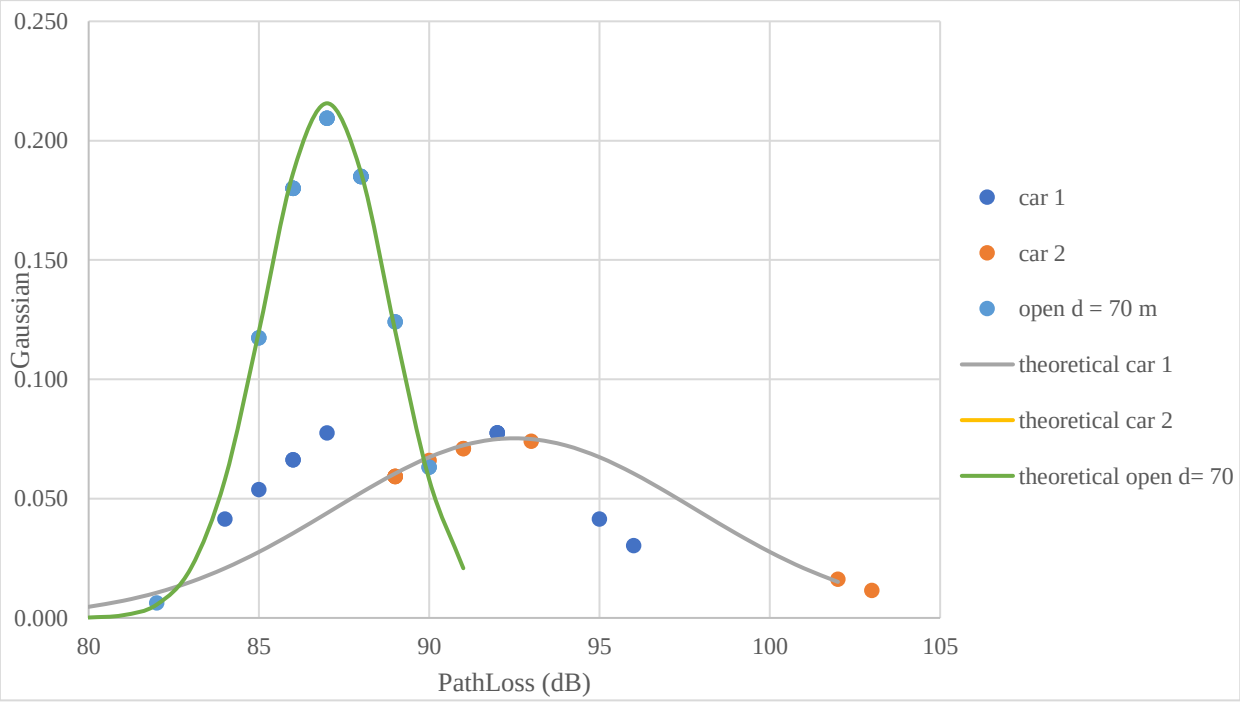

Fig. 20. Accuracy inside the car

In Fig. 20 it is seen that the experimental values of the normal distribution of the path loss, the mean of path loss and the standard deviation is compared with the path loss of the experimental and the theoretical values are compared which shows that the models accuracy ranging between 90-99% when the signal source is placed inside the car and when the car is stationary.

3. Theoretical model

The theoretical model was developed based on the log-normal model.

3.1 Model development

The receiver signal power (in SI units):

$$P_{RX} = \frac{G_{TX}G_{RX}P_{TX}}{L}; \quad (12)$$

where G_{TX}, G_{RX}, P_{TX}, are the transmitter, receiver gain and the transmitter power, respectively.

L is the propagation losses in the radio channel:

$$L = L_p L_S L_F. \quad (13)$$

Where L_p is path losses; L_S is shadowing losses; L_F is fast fading losses.

Then:

$$L_{[dBm]} = 10\lg L_p + 10lgL_S + 10lgL_F. \quad (14)$$

L_S is described by log-normal or normal distribution. Probability density function (PDF_N) of normal distribution is:

$$PDF_N = \frac{1}{\sigma\sqrt{2\pi}} exp\left(\frac{(x-\mu)^2}{2\sigma^2}\right) \quad . \quad (15)$$

Where x is true received signal level; μ is the average (mean) signal level; σ is standard deviation.

Log-normal $PDF_{L\text{-}N}$:

$$PDF_{L-N} = \frac{1}{\sigma\sqrt{2\pi}} exp\left(\frac{(X-M)^2}{2\sigma^2}\right). \quad (16)$$

Where, $X = 10lgx$; M is mean of X.

When receiver is far from transmitter, LF is described by Rayleigh distribution. PDF_R for Rayleigh is:

$$PDF_R = \frac{r}{\sigma^2} exp\left(-\frac{r^2}{2\sigma^2}\right), \; r \geq 0. \quad (17)$$

Here σ is standard deviation; r is the envelope of fading signal (amplitude of receiver signal). Middle value r_m of envelope signal which sample range to be satisfied by:

$$r_m = 1.777\sigma. \quad (18)$$

When receiver is close to transmitter, the envelope distribution of the received signal is Rician distribution. Then PDF_{Ric}:

$$PDF_{Ric} = \frac{r}{\sigma^2} exp\left(\frac{r^2+\alpha^2}{2\sigma^2}\right) \cdot I_0\left(\frac{r\cdot\alpha}{\sigma}\right), r \geq 0. \quad (19)$$

Here $I_0(X)$ is the zero-order Bessel function of the first kind; α is the amplitude of the dominant signal (LOS signal).

Most authors use the log-normal model as the main path losses model:

$$L_p = L_p(d_0) + 10nlg\left(\frac{d}{d_0}\right). \quad (20)$$

Where d is the direct distance between transmitter and receiver, d_0 is short distance from the transmitter, n is the path loss exponent estimated by linear regression. $L_p(d_0)$ is usually expressed as the free space path loss or the free-space path loss plus the accumulative antenna gain.

Shadowing effect is estimated by parameter X_σ, which is zero-mean normal distributed random variable with standard deviation σ and possibly with some time correlation. Then the equation (20) will look like this:

$$L_p = L_p(d_0) + 10nlg\left(\frac{d}{d_0}\right) + X_\sigma . \quad (21)$$

$$X_\sigma = 10\sum_{i=1}^{N} logX_i \sim N(0, \sigma^2) . \quad (22)$$

Most of the work involved in estimating the signal propagation of the VANET network is limited to that. That is, evaluate only large-scale fading. We were unable to find any work that assessed both large-scale fading and small-scale fading effects.

The proposed model is based on log-normal pass losses and evaluates all those effects:

. $$L_p = L_p(d_0) + 10nlg\left(\frac{d}{d_0}\right) + X_\sigma + X_F \quad (23)$$

Here X_F evaluates small scale fading.

X_σ evaluation. X_σ can be expressed in several ways:

1. $\boldsymbol{X_\sigma = N(0, \sigma)}$ Normal distribution. Usually, $\boldsymbol{2 \le \sigma \le 12}$;
2. The shadowing variance σ^2 is obtained by determining the MSE (mean square error) of the data versus the empirical path loss model with the minimizing the path loss exponent n:
   $\boldsymbol{\sigma = \sqrt{\frac{1}{N}\sum_{i=1}^{N}[L_{measures}(d_i) - L_{model}(d_i)]^2}}$, when L_{model} is expressed by equation (20).
3. $\boldsymbol{X_\sigma = e^{-\frac{\sigma^2}{2}+\sigma N}}$, where N is standard (0,1) normal random variable.

In this model we used $X_\sigma = N(0, \sigma)$. Then equation (21) becomes:

$$L_p = L_p(d_0) + 10nlg\left(\frac{d}{d_0}\right) + N(0, \sigma) \quad (24)$$

X_F evaluation. The X_F rating will depend on how far away the transmitter is from the receiver, i.e., whether we have a Rayleigh or a Rice distribution.

If the distance between the transmitter and receiver is small, then X_F can be described as follows:

$$X_F = N(\alpha, \sigma) \quad (25)$$

Where α is the dominant signal (see eq. (19)). We assume that "short distance" means a distance of up to 50 m. This will need to be confirmed experimentally.

We use the normal distribution for the description of X_F because parameter α describes signal propagation under LOS conditions.

So, the model for the short distance looks like this:

$$L_p = L_p(d_0) + 10nlg\left(\frac{d}{d_0}\right) + N_\sigma(0,\sigma) + N_F(\alpha,\sigma). \quad (26)$$

3.2. Model Evaluation

The model evaluation plays an important role as it must be ensured that before further steps the model needs to be proven right and must be given proper values of fading which can validate the model to proceed for further experimentation and comparison with the model.

For evaluation, the reference data have been taken from articles from which data are manipulated from graphs and comparisons of the study in which data such as distance between transmitter and receiver, power of transmission, frequency which are extrapolated using a tool which gives the values when graph is inputted as image with which the values were taken.

The evaluations involved various conversions and were performed on two models which showed that the shadowing effects were well in the range, and which proves that the model developed is correct. Below are the graphs that were used to extrapolate the values for the evaluation.

An online extrapolating tool was used in which the axis was aligned, and the data of the origin axes were given as input for the plot digitalizes the image into a graph and the points are obtained. After which the points are converted into required values with which the calculation of the shadowing of the dataset is obtained.

The below table was taken from the reference article [30] in which the path loss is measured for the sidewalk which is seen in Fig. 21 in this scenario the distance was given as a log model from which the distance was converted for the calculation of the free space path losses (FSPL) with which the shadowing effect of the scenario is calculated which can be seen in table 1.

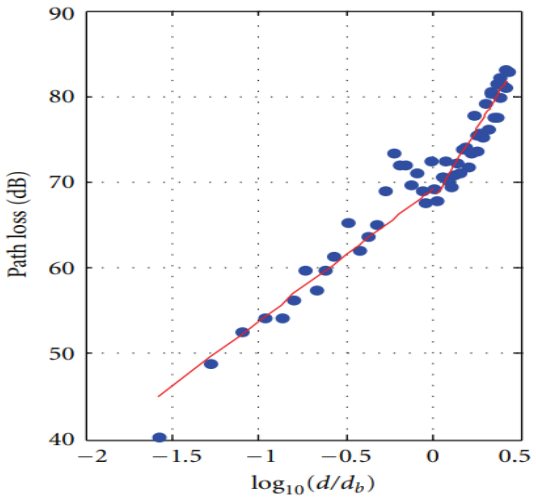

Fig. 21. Data points taken from article for evaluation which is a graph of path loss vs distance with two different scenarios [30].

Table 5. Calculation of FSPL and Shadowing effect on the scenario 1 from [30].

				Frequency (GHz)	*N*	
				2.45	1.99	
log(d/d_b)	Path loss	log *d*	*d* (m)	*FSPL*	10*n*log(d/d_0)	Shadowing effect (dB)
-1.57	40.32	0.006928	1.01	40.23	0.13	-0.0458
-1.27	48.89	0.299721	1.99	40.23	5.96	2.695
-1.10	52.47	0.472393	2.96	40.23	9.40	2.838
-0.97	54.09	0.607529	4.05	40.23	12.08	1.776
-0.87	54.09	0.705126	5.07	40.23	14.03	-0.165
-0.81	56.26	0.765186	5.82	40.23	15.22	0.808

From the above calculation it can be seen that the shadowing effect is well in the desired range as stated in the model formulation in this scenario. The table seen above has only the first 6 values the rest of the values can be seen in the appendix in which the whole table is shown.

The same was done to other scenario but the calculation process involved was different as in this case the distance was given but the power factor was in the power received so necessary conversion for the calculation were performed and the calculation can be seen in the table below the values were obtained from Fig. *22*.

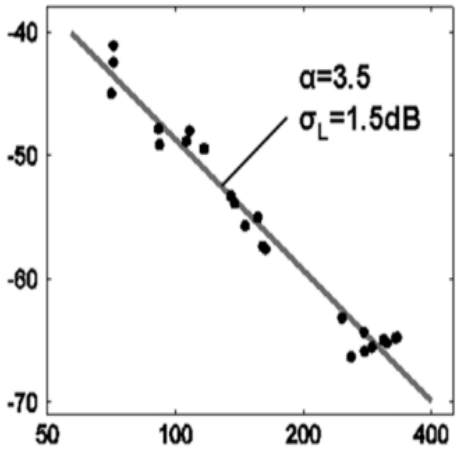

Fig. 22. Data points taken from article for evaluation which is a graph of path loss vs distance with two different scenarios [31].

Table 6. The FSPL and shadowing effect from the values taken from [31]

		For *PT*	*n*		
		18	1.489		
d (m)	*Pr* (dBm)	*PL* (dBm)	*FSPL*	10*n*log(d/d_0)	Shadowing effect (dB)
110.66	-40.98	58.98	40.23	30.43	-11.68
110	-42.32	60.32	40.23	30.39	-10.30
108.66	-44.71	62.71	40.23	30.31	-7.83
151.33	-47.46	65.46	40.23	32.45	-7.22
152.66	-48.73	66.73	40.23	32.51	-6.01
176.66	-48.52	66.52	40.23	33.46	-7.17

In this reference the shadowing effect were calculated for different transmission power with the received power data extracted from the graph with which the FSPL is also calculated. The remaining calculations are attached in the appendix with different transmission powers and for more data points.

4. Experimentation

The experimentation was performed with the hotspot, spectrum analyser and InSSIDer which are briefly discussed here.

4.1. Hotspot

Wi-Fi hotspot is the technology that allows internet access when away forms a network. They are like an alternate Wi-Fi connection which works on based on the location and the network from which the access is given. There are different types of Wi-Fi hotspots namely the public hotspot, mobile hotspot and prepaid hotspots. They all work differently. In this case using a mobile Wi-Fi hotspot in which the mobile's cellular data is used to create and share internet connectivity to which any other devices having Wi-Fi maybe connected. The hotspot configuration of the device that is used is from 802.11 a/b/g/n/ac are the protocols used with 2.45 GHz frequency. In this the carrier for network is operated in LTE mode with which the internet is shared between the vehicles and connected between two mobile devices.

4.2. Spectrum Analyser

Spectrum analyser will be used to calculate the signal parameters. It is used to analyse the spectrum of both known and unknown signals. In the analyser the most commonly used inputs are electrical, acoustic pressure waves can also be used when a transducer. There are two different types of spectrum analysers, Fast-Fourier Transform and swept-tuned analysers. The former uses a time sequence-based calculation while the later uses a super heterodyne receiver to down-convert a part of the input to centre frequency of a narrow band-pass filter whose instantaneous output power is recorded as a time function. The spectrum analysers show the values in which the basic bandwidths and the signals of input are set with which the output signal that's passed through can be seen in the screen of the analyser.

4.3. InSSIDer

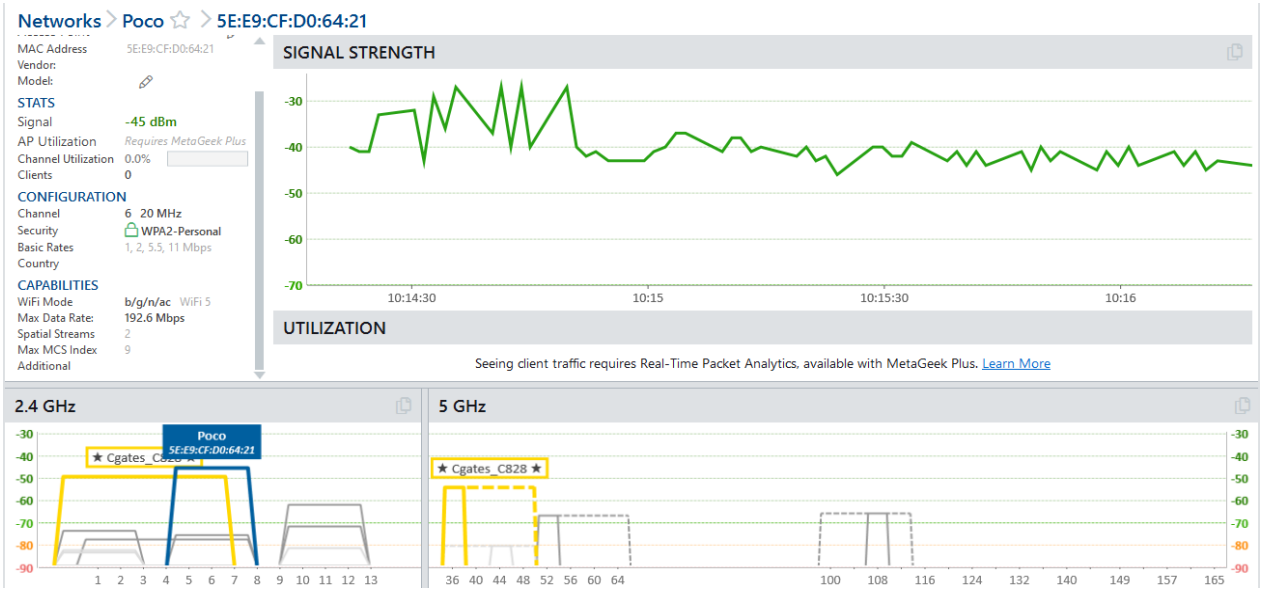

Fig. 23. InSSIDer results for the hotspot used

Similarly, there is a software in which the following values can be obtained called InSSIDer in which the various signals when connected to a Wi-Fi device can be seen and the results of an android phone hotspot can be seen in the Fig. 23 above. This can also be used in place of a spectrum analyser as the accuracy is almost similar to the spectrum analyser. This gives the details of whichever network it is connected to, so this is considered to be used for performing the experiments, as its user-friendly.

5. Results and Discussions

The results for the shadow fading and the fast fading are calculated for the various scenarios which were mentioned above. The theoretical and the experimental values of fast fading and shadow fading are obtained and compared with the graphs with which the graphs are constructed, and the values received which will be discussed in these sections. For the scenarios in which the cars are stationary only the path loss is calculated as fast fading has no effect when there is no movement in the cars and shadow fading is not considered as the location chosen for the obtaining the data was taken in open area without any obstructions the area in which the experiments were performed can be seen in the Fig. 24.

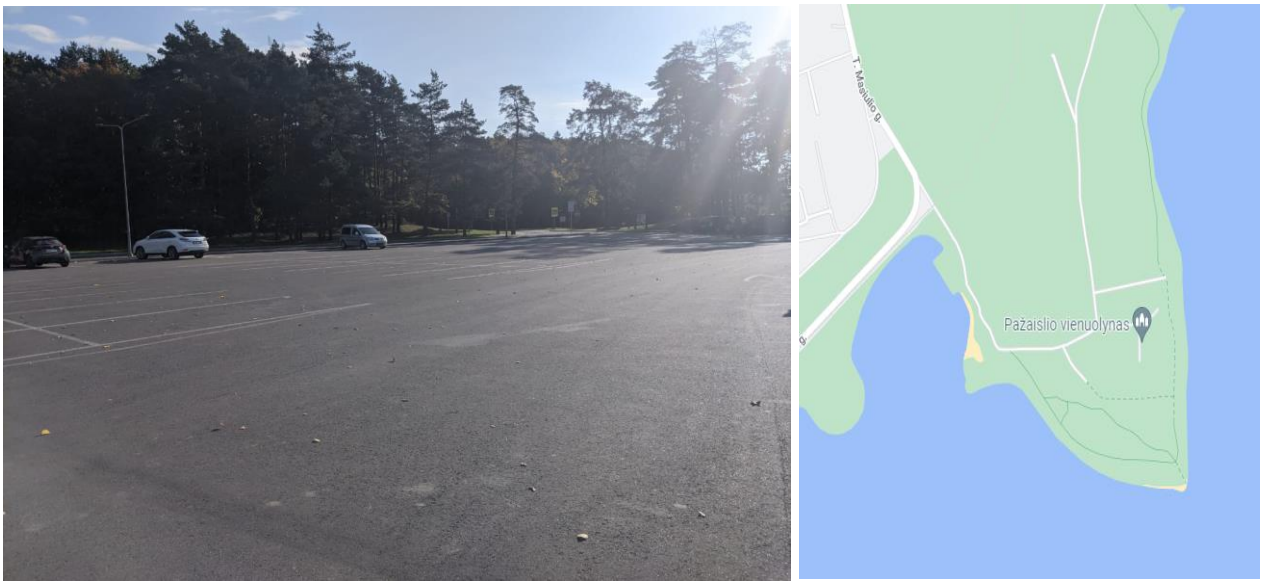

Fig. 24. Location in which the experiments were carried out.

5.1. When cars are one behind another

The first scenario as seen in Fig. 25, in which the cars are standing one behind another the values of path loss and the free space losses obtained at distances 50 m and 70 m for two cars. Here, the values obtained at 70m for both the cars are included the rest of the values can be seen in the appendix. The shadow fading is also calculated in this case since the weather was windy and there would be signal losses in such conditions so the shadow fading when the cars are parked are also measured.

Fig. 25. Cars one behind another

Table 7. Values of car parked side by side

		Car 1					Car 2			
d	P_R	*PL*	*FSPL*	10log(d/d_0)	Shadowing effect (dB)	P_R	*PL*	*FSPL*	10log(d/d_0)	Shadowing effect (dB)
70	-72	82	40.23	36.90	4.86	-71	81	40.2	36.902	3.86472
70	-75	85	40.23	36.90	7.86	-70	80	40.2	36.902	2.86472
70	-67	77	40.23	36.90	-0.14	-71	81	40.2	36.902	3.86472
70	-72	82	40.23	36.90	4.86	-69	79	40.2	36.902	1.86472
70	-66	76	40.23	36.90	-1.14	-69	79	40.2	36.902	1.86472
70	-72	82	40.23	36.90	4.86	-69	79	40.2	36.902	1.86472
70	-65	75	40.23	36.90	-2.14	-69	79	40.2	36.902	1.86472
70	-66	76	40.23	36.90	-1.14	-82	92	40.2	36.902	14.8647
70	-76	86	40.23	36.90	8.86	-73	83	40.2	36.902	5.86472
70	-64	74	40.23	36.90	-3.14	-83	93	40.2	36.902	15.8647

When cars are moving the readings were taken for each second and the distance was calculated based on the speed of the car which was 20 km/h covering 70 m distance for which the shadow fading, and the fast-fading results were obtained. The fast-fading comparison to theoretical and obtained values can be seen in the plot below in which the values correspond almost to the values of the theoretical calculations which is drawn as a trend line with the equation of the line which can be seen in the plot below in Fig. *26* and Fig. *27*.

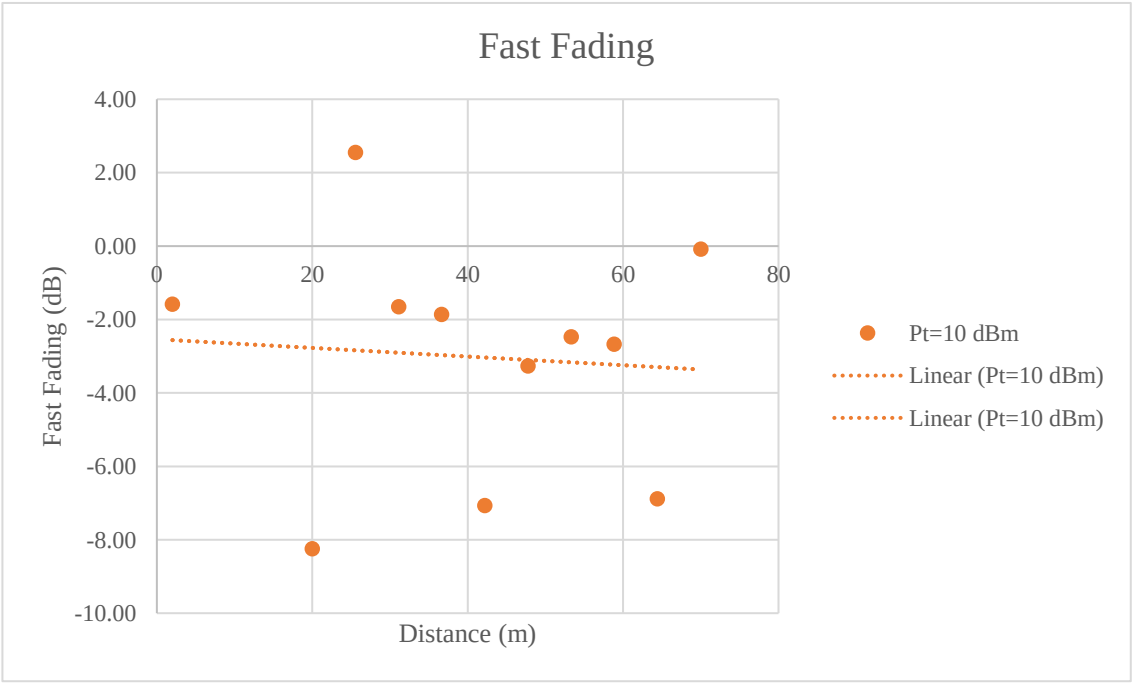

Fig. 26. Fast fading effect in car 1.

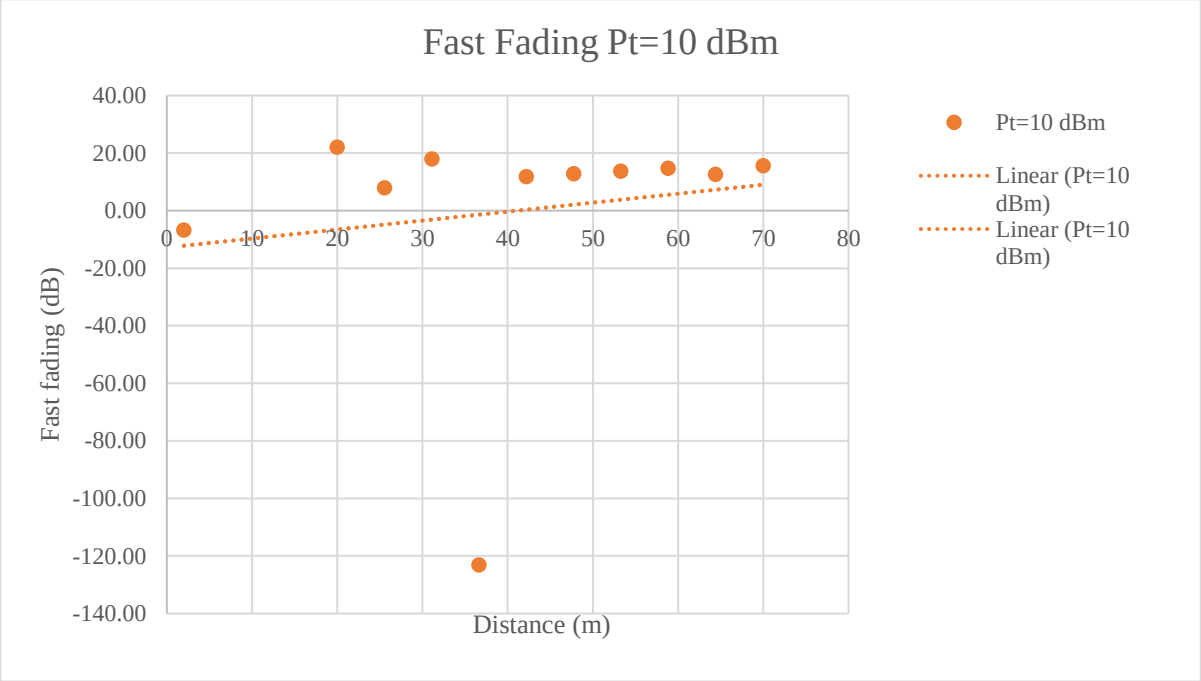

Fig. 27. Fast fading effect in car 2.

Here from the above two plots, it can be clearly noticed that the fast fading effect when the car moves one behind another are high within the 50m and after which the fast fading effects seem to decrease. This states that the shadowing effects seem to increase as the distance increase. The values that were obtained are all seen in the appendix.

5.2. When cars are against each other

In this case the cars face each other as shown in Fig. 28 and the readings are taken at 70 m. Since the weather conditions were same in this scenario the shadow fading was also calculated when the cars were parked and the calculation for both shadow fading and the fast fading was done in the case of moving for both the cars. The table below shows the values when cars are stationary, and the plots show the fast fading of the cars when they are on the run.

Fig. 28. Cars against each other.

Table 8. Calculation when cars are moving against each other.

		Car 1					Car 2			
d	P_R	*PL*	*FSPL*	10log(d/d_0)	Shadowing effect (dB)	P_R	*PL*	*FSPL*	10*n*log(d/d_0)	Shadowing effect (dB)
70	-55	65	40.23	36.90	-12.14	-55	65	40.2	36.90	-12.14
70	-63	73	40.23	36.90	-4.14	-56	66	40.2	36.90	-11.14
70	-62	72	40.23	36.90	-5.14	-58	68	40.2	36.90	-9.14
70	-62	72	40.23	36.90	-5.14	-63	73	40.2	36.90	-4.14
70	-65	75	40.23	36.90	-2.14	-70	80	40.2	36.90	2.86
70	-56	66	40.23	36.90	-11.14	-65	75	40.2	36.90	-2.14
70	-67	77	40.23	36.90	-0.14	-69	79	40.2	36.90	1.86
70	-68	78	40.23	36.90	0.86	-60	70	40.2	36.90	-7.14
70	-62	72	40.23	36.90	-5.14	-53	63	40.2	36.90	-14.14
70	-59	69	40.23	36.90	-8.14	-67	77	40.2	36.90	-0.14

The readings when the cars are moving are also calculated and the plots of the fast fading for this scenario can be seen in the figure below. The distances and the readings were performed in the same manner as the previous scenario. Fig. 29 and Fig. 30 shows the fast fading in scenario 2.

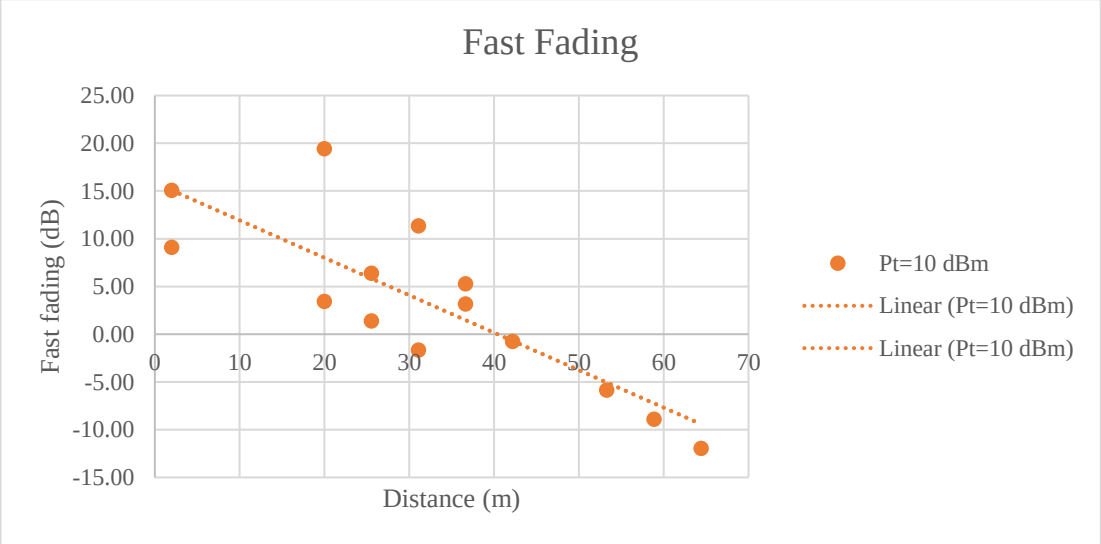

Fig. 29. Fast fading in car 2.

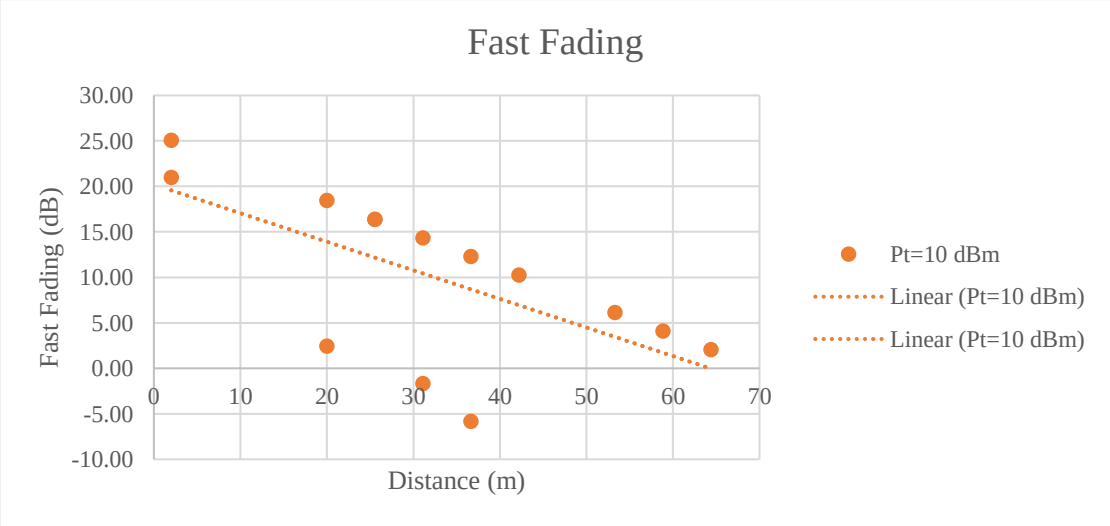

Fig. 30. Fast fading in car 2

The above two plots, it can be clearly noticed that the fast fading effect when the car moves against each other are soaring when the distance is up to 50m and after which the fast fading effects seem to decrease bringing the shadowing effects to be predominant, the values of these can be noticed in the appendix.

5.3. Cars in parallel (side by side)

As shown in Fig. 31 below the cars are parked in parallel and the values were calculated in the same conditions as mentioned in the previous two scenarios.

Fig. 31. Cars facing front in parallel.

Table 9. Fading when cars are parked in parallel

		Car 1					Car 2			
d	P_R	*PL*	*FSPL*	10log(d/d_0)	Shadowing effect	P_R	*PL*	*FSPL*	10log(d/d_0)	Shadowing effect (dB)
70	-65	75	40.23	36.90	-2.14	-65	75	40.2	36.90	-2.14
70	-68	78	40.23	36.90	0.86	-70	80	40.2	36.90	2.86
70	-67	77	40.23	36.90	-0.14	-68	78	40.2	36.90	0.86
70	-66	76	40.23	36.90	-1.14	-66	76	40.2	36.90	-1.14
70	-66	76	40.23	36.90	-1.14	-67	77	40.2	36.90	-0.14
70	-68	78	40.23	36.90	0.86	-62	72	40.2	36.90	-5.14
70	-68	78	40.23	36.90	0.86	-68	78	40.2	36.90	0.86
70	-70	80	40.23	36.90	2.86	-66	76	40.2	36.90	-1.14
70	-66	76	40.23	36.90	-1.14	-67	77	40.2	36.90	-0.14
70	-69	79	40.23	36.90	1.86	-69	79	40.2	36.90	1.86

The results of fast fading when the cars move parallel to a point is seen in the below plots Fig. 32 and **Fig. *33***.

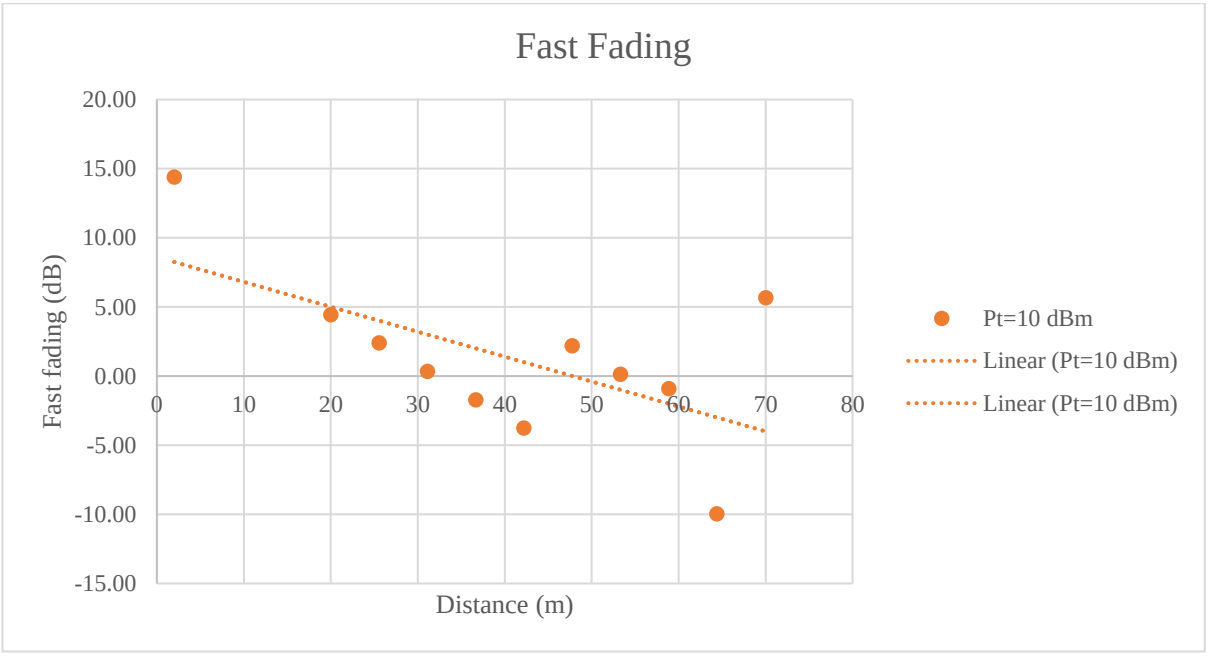

Fig. 32. Fast fading in first car.

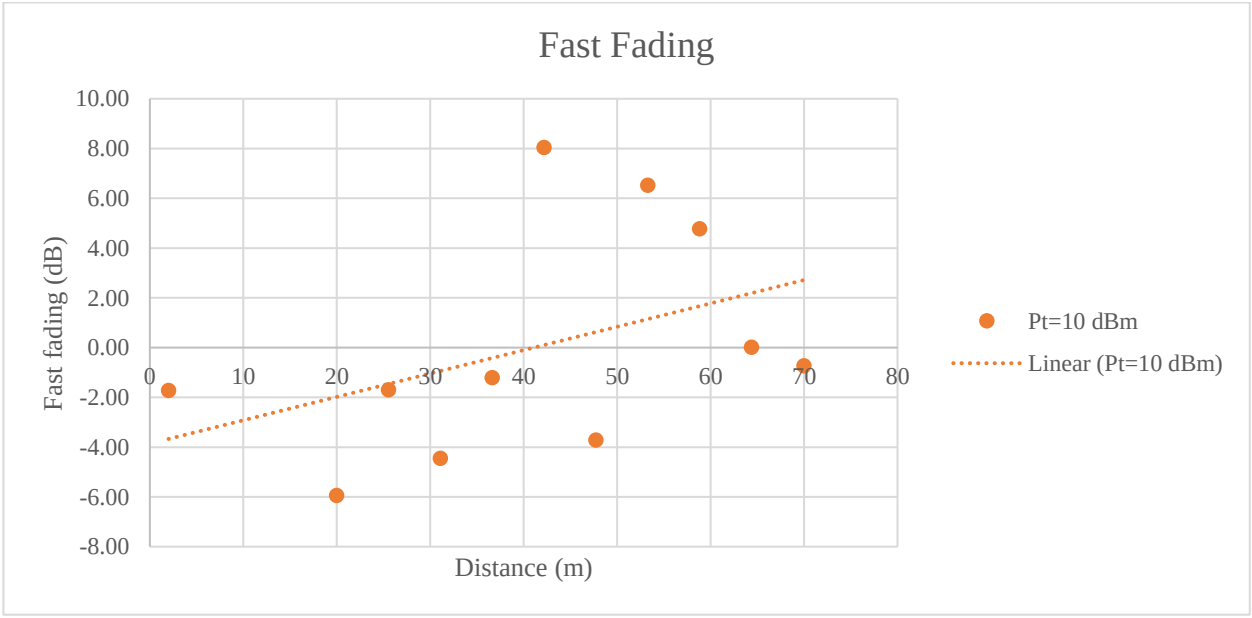

Fig. 33. Fast fading when cars move parallelly towards a point

The above two plots, it can be clearly noticed that the fast fading effect when the cars move side by side parallelly, are increasing when the distance is up to 50m, beyond which the fast fading effects seem to decline bringing the shadowing effects to be major, the values of these can be seen in the appendix section.

5.4. Interpretations of the results

The results above shows that the effect of fast fading has varying effects on different scenarios. From the results obtained there is effective fast-fading effect in all the scenarios that is affected due to the surrounding and the environmental conditions which is dependent on the distance. Noticeably when the distance is beyond 50m the fast fading effect diminishes and the shadowing effect dominates and until 50m distance the fast fading effect predominates.

So the model must be altered according to the findings from the results.

If the distance is large (assumed d > 50 m), the then X_F can be described as follows:

$$X_F = N(0, \sigma) \, . \tag{27}$$

Such a choice follows from the definition of the Rayleigh distribution.

So, the model for the large distance is written as such:

$$L_p = L_p(d_0) + 10nlg\left(\frac{d}{d_0}\right) + N_\sigma(0,\sigma) + N_\sigma(0,\sigma) = L_p(d_0) + 10nlg\left(\frac{d}{d_0}\right) + 2N_\sigma(0,\sigma). \tag{28}$$

Thus, by summarizing equations (26) and (28), the model can be written in the following manner:

$$. \qquad L_p = \begin{cases} L_p(d_0) + 10nlg\left(\frac{d}{d_0}\right) + N_\sigma(0,\sigma) + N_F(\alpha,\sigma), & if\ d \le 50\ m \\ L_p(d_0) + 10nlg\left(\frac{d}{d_0}\right) + 2N_\sigma(0,\sigma) & if\ \ d > 50\ m \end{cases} . \tag{29}$$

In the above scenario the experiments were performed on a windy and a clear day on which from the computed results there is effect of fast fading even when the cars are stationary. But there are no considerable changes in the fast fading in the stationary cases, when the cars are in movement it can be clearly seen that the fast-fading effect can be seen from the plots above which says that the while experimentally performed there is a dependency of distance that plays a major role with which it is concluded that when the distance is less than 50 m, the amplitude of the dominant signal is considered whereas at distances greater than 50 m the normal distribution of the path loss is considered.

Conclusion

1. An analysis of the literature has shown that the vast majority of models for the VANET network do not evaluate the fast fading caused by the movement of vehicles.

2. After analysis of the literature, it was decided to adopt a log-normal model as the basic model, as it evaluates both the signal propagation environment and the slow fading (shadowing effect).

3. A mathematical model based on the log-normal signal propagation prediction model and the experimental results of two other authors are proposed in the work.

4. In this work, experiments were performed to adjust the developed model. Methodological measurements showed the error was observed to be a maximum of 8.7 % when signal source was in open area and 10 % when placed inside the car. The average error rate of the model was calculated to be 3.1% which shows an accuracy rate of 96.9 % for the values obtained using the developed model.

5. Experiments have shown that both slow fading and fast fading are observed at a distance between moving cars of less than 50 m. When the distance is greater than 50 m, slow fading predominates.

6. Based on the experiments, the theoretical model was adjusted. As a final model, a model is proposed, which is represented in the work by a equation (29).

References

[1] The Impact of Inter-Vehicle Communication . Killat, Moritz. Hamburg : KIT Scientific Publishing, 2009. ISBN 978-3-86644-445-4.

[2] Vehicular ad hoc Networks. Campolo, Claudia and Molinaro, Antonella and Scopigno, Riccardo. s.l. : Springer, 2015. ISBN 978-3-319-15496-1.

[3] Annoni, M., & Williams, B. The history of vehicular networks. [book auth.] C., Molinaro, A., & Scopigno, R. Campolo. Vehicular ad hoc Networks. s.l. : Springer, 2015.

[4] Fischer, Hans-Joachim. Standardization and Harmonization Activities. [book auth.] C., Molinaro, A., & Scopigno, R. Campolo. Vehicular ad hoc Networks. s.l. : Springer, 2015.

[5] Riccardo M. Scopigno, Alessia Autolitano, and Weidong Xiang. The Physical Layer of VANETs. [book auth.] C., Molinaro, A., & Scopigno, R. Campolo. Vehicular ad hoc Networks. s.l. : Springer, 2015.

[6] What is offered traffic in a real telecommunication network. Poryazov, S. A. Beijing, China : 19th International Teletraffic Congress,, 2005.

[7] Poryazov, S. A., & Saranova, E. T. Some general terminal and network teletraffic equations for virtual circuit switching systems. Modeling and Simulation Tools for Emerging Telecommunication Networks (pp.471-505). Boston, MA : Springer, 2006.

[8] V2V communication channels: State of knowledge, new results, and what's next. Matolak, David W. Berlin, Heidelberg : Springer, 2013.

[9] Design of Shark Fin Integrated Antenna Systems for Automotive Applications. Demien, C., & Sarkis, R. Rome, Italy : In 2019 PhotonIcs & Electromagnetics Research Symposium-Spring (PIERS-Spring), 2019.

[10] Analysis of low cost communication technologies for V2I applications. . Martinez, A., Canibano, E., & Romo, J. Valladolid, Spain : MDPI, 2020.

[11] Vehicular ad hoc networks: architectures, research issues, methodologies, challenges, and trends. Liang, W., Li, Z., Zhang, H., Wang, S., & Bie, R. s.l. : International Journal of Distributed Sensor Networks, Hindawi Publishing Coperation, 2015.

[12] Mahmood, Zaigham. Connected Vehicles in the Internet of Things. s.l. : Springer Nature Switzerland AG, 2020. 978-3-030-36167-9.

[13] Performance Evaluation of V2V and V2R Communication Based on 2-Wavelength Cognitive Wireless Network on Road State Information GIS Platform. Sakuraba, A., Shibata, Y., Sato, G., & Uchida, N. Cham : In International Conference on Intelligent Networking and Collaborative Systems, Springer, 2019. 978-3-030-29035-1_21.

[14] Distance dependence of path loss for millimeter wave inter-vehicle communications. Takahashi, S., Kato, A., Sato, K., & Fujise, M. Yokosuka : IEEE 58th Vehicular Technology Conference., 2003.

[15] Modeling on impact of metal object obstruction in urban environment for internet of things application in vehicular communication. Turner, J. S. C., Harun, A., Yasin, M. N. M., Ali, N., Bakar, S. A., Fadzilla, M. A., ... & Phoon, C. Y. s.l. : AIP Conference Proceedings 2203, 020053 (2020), 2020.

[16] Vehicle mobility and communication channel models for realistic and efficient highway VANET simulation. Akhtar, N., Ergen, S. C., & Ozkasap, O. s.l. : IEEE Transactions on Vehicular Technology, 64(1), 248-262., 2014.

[17] Unified stochastic geometry modeling and analysis of cellular networks in LOS/NLOS and shadowed fading. Trigui, I., Affes, S., & Liang, B. s.l. : IEEE Transactions on Communications, 65(12), 5470-5486., 2017.

[18] Boban, M. Realistic and efficient channel modeling for vehicular networks. Pittsburgh : Doctoral dissertation, Carnegie Mellon University, 2012.

[19] Shadow Fading Model for Vehicle-to-Vehicle Network Simulators. Abbas, T., Tufvesson, F., Sjoberg, K., & Karedal, J. Lund : COST IC1004 5th Management Committee and Scientific Meeting, 2012.

[20] The Optimal Radio Propagation Model in VANET. Hafeez, K. A., Zhao, L., Liao, Z., & Ma, B. N. W. Ontario : In Fourth International Conference on Systems and Networks Communications (pp. 6-11). IEEE., 2009.

[21] Fast Fading Mobile Channel Modeling For wireless . Lavanya, V., Rao, G. S., & Bidikar, B. s.l. : Procedia Computer Science, 2016.

[22] Discrete Rayleigh fading channel modeling. Aráuz, J., Krishnamurthy, P., & Labrador, M. A. s.l. : Wireless Communications and Mobile Computing, 4(4), 413-425, 2004.

[23] Assessing the Impact of a Realistic Radio Propagation Model on VANET Scenarios using Real Maps. Martinez, F. J., Fogue, M., Coll, M., Cano, J. C., Calafate, C. T., & Manzoni, P. s.l. : In 2010 Ninth IEEE International Symposium on Network Computing and Applications (pp. 132-139). IEEE., 2010.

[24] An environmental channel throughput and radio propagation modeling for vehicle-to-vehicle communication. Al-Absi, M. A., Al-Absi, A. A., Kim, T., & Lee, H. J. 4, s.l. : International Journal of Distributed Sensor Networks, 2018, Vol. 4.

[25] A survey of propagation models used in vehicular ad hoc network (vanet) research. Van Eenennaam, E. M. s.l. : Paper written for course Mobile Radio Communication, Universtiy of Twente, 2008, Vol. 46.

[26] A lightweight radio propagation model for vehicular communication in road tunnels. Qureshi, M. A., Noor, R. M., Shamim, A., Shamshirband, S., & Raymond Choo, K. K. 3, s.l. : PloS one, 2016, Vol. 11.

[27] Chandrasekharamenon, N. P., & AnchareV, B. Chandrasekharamenon, N. P., & AnchareV, B. s.l. : EURASIP Journal on Wireless Communications and Networking , 2012. 1687-1499-2012-1.

[28] A realistic path loss model for real-time communication in the urban grid environment for Vehicular Ad hoc Networks. Mostajeran, E., Noor, R. M., Anisi, M. H., Ahmedy, I., & Khan, F. A. s.l. : KSII Transactions on Internet and Information Systems, Korea Society of Internet Information, 2017, Vol. 11.

[29] tudying the impact of the CORNER propagation model on VANET routing in urban environments. Mukunthan, A., Cooper, C., Safaei, F., Franklin, D., & Abolhasan, M. Wollongong : IEEE Vehicular Technology Conference (VTC Fall), 2012. 978-1-4673-1881-5.

[30] Near-ground path loss measurements and modeling for wireless sensor networks at 2.4 GHz. Wang, D., Song, L., Kong, X., & Zhang, Z. Taiyuan : International Journal of Distributed Sensor Networks, 2012.

[31] Path-loss characteristics of urban wireless channels. Herring, K. T., Holloway, J. W., Staelin, D. H., & Bliss, D. W. 1, s.l. : IEEE Transactions on Antennas and Propagation, 2010, Vol. 58.

Appendix

Calculation for the first literature [30] extracted data:

				Frequency (GHz)	n		
				2.45	1.99		
log(d/db)	Path loss	log d	d(m)	FSPL	10nlog(d/d0)	Shadowing effect (dB)	Fast Fading (dB)
-1.57	40.33	0.01	1.016	40.233	0.138	-0.046	40.371
-1.28	48.89	0.30	1.994	40.233	5.964	2.696	46.198
-1.11	52.47	0.47	2.968	40.233	9.401	2.839	49.634
-0.97	54.10	0.61	4.051	40.233	12.090	1.777	52.323
-0.87	54.10	0.71	5.071	40.233	14.032	-0.166	54.265
-0.81	56.27	0.77	5.824	40.233	15.227	0.808	55.461
-0.68	57.35	0.90	7.949	40.233	17.916	-0.796	58.150
-0.74	59.63	0.84	6.922	40.233	16.721	2.677	56.955
-0.63	59.74	0.95	8.818	40.233	18.813	0.694	59.046
-0.57	61.26	1.01	10.126	40.233	20.008	1.017	60.241
-0.43	62.02	1.15	14.063	40.233	22.847	-1.063	63.080
-0.39	63.64	1.19	15.600	40.233	23.743	-0.332	63.976
-0.50	65.27	1.08	12.037	40.233	21.502	3.536	61.735
-0.33	65.05	1.25	17.606	40.233	24.789	0.032	65.022
-0.06	67.66	1.52	33.377	40.233	30.317	-2.893	70.550
0.01	67.87	1.59	38.995	40.233	31.661	-4.020	71.894
-0.07	68.96	1.51	32.243	40.233	30.018	-1.292	70.251
-0.14	69.61	1.44	27.597	40.233	28.673	0.703	68.906
-0.29	68.96	1.29	19.530	40.233	25.685	3.040	65.918
0.00	69.18	1.58	37.670	40.233	31.362	-2.420	71.596
0.09	69.39	1.67	47.162	40.233	33.305	-4.145	73.538
0.09	70.04	1.67	46.354	40.233	33.155	-3.345	73.388
0.04	70.59	1.62	41.787	40.233	32.259	-1.906	72.492
0.10	70.69	1.68	47.985	40.233	33.454	-2.993	73.687
0.15	71.02	1.73	53.229	40.233	34.350	-3.564	74.584
0.19	71.78	1.77	59.046	40.233	35.247	-3.701	75.480
0.13	72.21	1.71	51.420	40.233	34.052	-2.072	74.285
0.06	72.43	1.64	43.257	40.233	32.558	-0.361	72.791
-0.02	72.54	1.56	36.390	40.233	31.064	1.241	71.297
-0.10	71.02	1.48	30.088	40.233	29.420	1.366	69.653
-0.17	72.00	1.41	25.753	40.233	28.076	3.687	68.309
-0.20	72.00	1.38	24.033	40.233	27.478	4.284	67.711
-0.23	73.41	1.35	22.427	40.233	26.880	6.292	67.114
0.15	73.84	1.73	54.157	40.233	34.500	-0.894	74.733
0.20	73.41	1.78	60.076	40.233	35.396	-2.224	75.629
0.24	73.73	1.82	65.499	40.233	36.143	-2.645	76.376
0.18	74.16	1.76	57.040	40.233	34.948	-1.016	75.181
0.27	75.14	1.85	71.413	40.233	36.890	-1.982	77.123
0.24	75.57	1.82	65.499	40.233	36.143	-0.802	76.376
0.28	76.01	1.86	72.658	40.233	37.040	-1.264	77.273

0.31	76.23	1.89	77.860	40.233	37.637	-1.645	77.870
0.22	77.85	1.80	63.274	40.233	35.844	1.775	76.078
0.34	77.64	1.92	83.434	40.233	38.235	-0.832	78.468
0.28	79.15	1.86	72.658	40.233	37.040	1.881	77.273
0.32	80.46	1.90	79.217	40.233	37.787	2.436	78.020
0.39	79.80	1.97	92.552	40.233	39.131	0.440	79.364
0.35	81.43	1.93	84.889	40.233	38.384	2.814	78.617
0.42	81.00	2.00	99.178	40.233	39.729	1.036	79.962
0.37	81.97	1.95	89.407	40.233	38.832	2.908	79.066
0.39	82.52	1.97	92.552	40.233	39.131	3.152	79.364
0.41	83.06	1.99	97.479	40.233	39.579	3.246	79.813
0.44	82.84	2.02	104.458	40.233	40.177	2.431	80.410

Calculation for second literature [31] with different transmission power with 2.45GHz frequency

		For PT	n			
		18	1.489			
d(m)	Pr (dBm)	PL(dBm)	FSPL	10nlog(d/d0)	Shadowing effect (dB)	Fast fading (dB)
110.67	-40.99	58.99	40.23	30.44	-11.68	70.67
110.00	-42.32	60.32	40.23	30.40	-10.31	70.63
108.67	-44.72	62.72	40.23	30.32	-7.83	70.55
151.33	-47.46	65.46	40.23	32.46	-7.23	72.69
152.67	-48.73	66.73	40.23	32.52	-6.02	72.75
176.67	-48.52	66.52	40.23	33.46	-7.17	73.69
180.00	-47.75	65.75	40.23	33.58	-8.07	73.81
192.67	-49.08	67.08	40.23	34.02	-7.17	74.25
218.00	-52.82	70.82	40.23	34.82	-4.24	75.05
221.33	-53.38	71.38	40.23	34.92	-3.77	75.15
230.00	-55.07	73.07	40.23	35.17	-2.33	75.40
241.33	-54.51	72.51	40.23	35.48	-3.20	75.71
246.00	-56.69	74.69	40.23	35.60	-1.14	75.83
248.67	-56.90	74.90	40.23	35.67	-1.00	75.90
318.67	-62.39	80.39	40.23	37.27	2.89	77.51
339.33	-63.52	81.52	40.23	37.68	3.61	77.91
327.33	-65.42	83.42	40.23	37.45	5.74	77.68
338.67	-65.00	83.00	40.23	37.67	5.10	77.90
345.33	-64.72	82.72	40.23	37.79	4.69	78.03
356.67	-64.08	82.08	40.23	38.00	3.85	78.24
360.00	-64.37	82.37	40.23	38.06	4.07	78.30
366.00	-63.94	81.94	40.23	38.17	3.54	78.40
368.00	-63.80	81.80	40.23	38.21	3.36	78.44

		For PT 20				
d(m)	Pr (dBm)	PL(dBm)	FSPL	10nlog(d/d0)	Shadowing effect (dB)	Fast Fading (dB)
110.67	-40.99	60.99	40.23	30.44	-9.68	70.67
110.00	-42.32	62.32	40.23	30.40	-8.31	70.63
108.67	-44.72	64.72	40.23	30.32	-5.83	70.55
151.33	-47.46	67.46	40.23	32.46	-5.23	72.69
152.67	-48.73	68.73	40.23	32.52	-4.02	72.75
176.67	-48.52	68.52	40.23	33.46	-5.17	73.69
180.00	-47.75	67.75	40.23	33.58	-6.07	73.81
192.67	-49.08	69.08	40.23	34.02	-5.17	74.25
218.00	-52.82	72.82	40.23	34.82	-2.24	75.05
221.33	-53.38	73.38	40.23	34.92	-1.77	75.15
230.00	-55.07	75.07	40.23	35.17	-0.33	75.40
241.33	-54.51	74.51	40.23	35.48	-1.20	75.71
246.00	-56.69	76.69	40.23	35.60	0.86	75.83
248.67	-56.90	76.90	40.23	35.67	1.00	75.90
318.67	-62.39	82.39	40.23	37.27	4.89	77.51
339.33	-63.52	83.52	40.23	37.68	5.61	77.91
327.33	-65.42	85.42	40.23	37.45	7.74	77.68
338.67	-65.00	85.00	40.23	37.67	7.10	77.90
345.33	-64.72	84.72	40.23	37.79	6.69	78.03
356.67	-64.08	84.08	40.23	38.00	5.85	78.24
360.00	-64.37	84.37	40.23	38.06	6.07	78.30
366.00	-63.94	83.94	40.23	38.17	5.54	78.40
368.00	-63.80	83.80	40.23	38.21	5.36	78.44

Calculations for Accuracy evaluation when hotspot is placed in open area.

	F= 2.45 GHz	PTx= 10 dBm									
D m	P_R dBm	PL dBm	Mean dBm	σ^2 variance	σ	ΔPL (absolute error)	ΔPL mean	(ΔPL/PL)* 100% relative error	Gaussian	γ skew	Kurtosis
50	-67	77	79.4	9.31	3.05	2.4	2.38	3.12	0.10	0.78	0.52
50	-71	81	79.4		3.05	1.6		1.98	0.11		
50	-74	84	79.4		3.05	4.6		5.48	0.04		
50	-71	81	79.4		3.05	1.6		1.98	0.11		
50	-67	77	79.4		3.05	2.4		3.12	0.10		
50	-66	76	79.4		3.05	3.4		4.47	0.07		
50	-69	79	79.4		3.05	0.4		0.51	0.13		
50	-69	79	79.4		3.05	0.4		0.51	0.13		
50	-69	79	79.4		3.05	0.4		0.51	0.13		
50	-70	80	79.4		3.05	0.6		0.75	0.13		
50	-65	75	79.4		3.05	4.4		5.87	0.05		

50	-69	79	79.4		3.05	0.4		0.51	0.13
50	-66	76	79.4		3.05	3.4		4.47	0.07
50	-68	78	79.4		3.05	1.4		1.79	0.12
50	-73	83	79.4		3.05	3.6		4.34	0.07
50	-71	81	79.4		3.05	1.6		1.98	0.11
50	-72	82	79.4		3.05	2.6		3.17	0.09
50	-77	87	79.4		3.05	7.6		8.74	0.01
50	-66	76	79.4		3.05	3.4		4.47	0.07
50	-68	78	79.4		3.05	1.4		1.79	0.12

F= 2.45 GHz	PTx= 10 dBm

D m	P_R dBm	PL dBm	Mean dBm	σ^2 variance	σ	ΔPL (absolute error)	ΔPL mean	(ΔPL/PL)* 100% relative error	Gaussian	γ skew	Kurtosis
70	-65	75	77.05	3.63	1.90	2.05	1.455	2.73	0.12	-0.69	1.27
70	-68	78	77.05		1.90	0.95		1.22	0.18		
70	-67	77	77.05		1.90	0.05		0.06	0.21		
70	-66	76	77.05		1.90	1.05		1.38	0.18		
70	-66	76	77.05		1.90	1.05		1.38	0.18		
70	-68	78	77.05		1.90	0.95		1.22	0.18		
70	-68	78	77.05		1.90	0.95		1.22	0.18		
70	-70	80	77.05		1.90	2.95		3.69	0.06		
70	-66	76	77.05		1.90	1.05		1.38	0.18		
70	-69	79	77.05		1.90	1.95		2.47	0.12		
70	-65	75	77.05		1.90	2.05		2.73	0.12		
70	-70	80	77.05		1.90	2.95		3.69	0.06		
70	-68	78	77.05		1.90	0.95		1.22	0.18		
70	-66	76	77.05		1.90	1.05		1.38	0.18		
70	-67	77	77.05		1.90	0.05		0.06	0.21		
70	-62	72	77.05		1.90	5.05		7.01	0.01		
70	-68	78	77.05		1.90	0.95		1.22	0.18		
70	-66	76	77.05		1.90	1.05		1.38	0.18		
70	-67	77	77.05		1.90	0.05		0.06	0.21		
70	-69	79	77.05		1.90	1.95		2.47	0.12		

x	μ	σ2	σ	Gausian, d= 50 m
70	79.5	16.45	2.9	0.0006
71	79.5	16.45	2.9	0.0019
72	79.5	16.45	2.9	0.0049
73	79.5	16.45	2.9	0.0112
74	79.5	16.45	2.9	0.0228
75	79.5	16.45	2.9	0.0413
76	79.5	16.45	2.9	0.0664
77	79.5	16.45	2.9	0.0949
78	79.5	16.45	2.9	0.1203

x	μ	σ	Gausian, d = 70 m
70	77	1.9	0.0002
71	77	1.9	0.0014
72	77	1.9	0.0066
73	77	1.9	0.0229
74	77	1.9	0.0604
75	77	1.9	0.1207
76	77	1.9	0.1828
77	77	1.9	0.2100
78	77	1.9	0.1828

79	79.5	16.45	2.9	0.1355	79	77	1.9	0.1207
80	79.5	16.45	2.9	0.1355	80	77	1.9	0.0604
81	79.5	16.45	2.9	0.1203	81	77	1.9	0.0229
82	79.5	16.45	2.9	0.0949	82	77	1.9	0.0066
83	79.5	16.45	2.9	0.0664	83	77	1.9	0.0014
84	79.5	16.45	2.9	0.0413	84	77	1.9	0.0002
85	79.5	16.45	2.9	0.0228	85	77	1.9	2.97E-05
86	79.5	16.45	2.9	0.0112	86	77	1.9	2.82E-06
87	79.5	16.45	2.9	0.0049	87	77	1.9	2.03E-07
88	79.5	16.45	2.9	0.0019	88	77	1.9	1.11E-08
89	79.5	16.45	2.9	0.0006	89	77	1.9	4.57E-10
90	79.5	16.45	2.9	0.0002	90	77	1.9	1.43E-11

Calculations for accuracy evaluation when hotspot is placed inside the cars.

F=2.45 GHz	P_{TX}= 10 dBm

car 1												
D m	P_R dBm	PL dBm	Mean dBm	σ^2 variance	σ	ΔPL (absolute error)	ΔPL mean	(ΔPL/PL)* 100% relative error	Gaussian	γ skew	Kurtosis	open-car mean dBm
70	-72	92	89.5	19.167	4.38	2.5	3.9	2.72	0.077	0.21	-1.68	-2.45
70	-75	95	89.5		4.38	5.5		5.79	0.041			
70	-67	87	89.5		4.38	2.5		2.87	0.077			
70	-72	92	89.5		4.38	2.5		2.72	0.077			
70	-66	86	89.5		4.38	3.5		4.07	0.066			
70	-72	92	89.5		4.38	2.5		2.72	0.077			
70	-65	85	89.5		4.38	4.5		5.29	0.054			
70	-66	86	89.5		4.38	3.5		4.07	0.066			
70	-76	96	89.5		4.38	6.5		6.77	0.030			
70	-64	84	89.5		4.38	5.5		6.55	0.041			

Car 2												
D m	P_R dBm	PL dBm	Mean dBm	σ^2 variance	σ	ΔPL (absolute error)	ΔPL mean	(ΔPL/PL) * 100% relative error	Gaussian	γ skew	Kurtosis	open-car (mean), dBm
70	-71	91	92.6	28.93	5.38	1.6	4.04	1.76	0.07	-1.19	0.94	-5.55
70	-70	90	92.6		5.38	2.6		2.89	0.07			
70	-71	91	92.6		5.38	1.6		1.76	0.07			
70	-69	89	92.6		5.38	3.6		4.04	0.06			
70	-69	89	92.6		5.38	3.6		4.04	0.06			
70	-69	89	92.6		5.38	3.6		4.04	0.06			
70	-69	89	92.6		5.38	3.6		4.04	0.06			
70	-82	102	92.6		5.38	9.4		9.22	0.02			
70	-73	93	92.6		5.38	0.4		0.43	0.07			
70	-83	103	92.6		5.38	10.4		10.10	0.01			

x	μ	σ	Gausian, d = 70 m
80	92.5	5.3	0.0047
81	92.5	5.3	0.0071
82	92.5	5.3	0.0106
83	92.5	5.3	0.0151
84	92.5	5.3	0.0208
85	92.5	5.3	0.0277
86	92.5	5.3	0.0355
87	92.5	5.3	0.0439
88	92.5	5.3	0.0525
89	92.5	5.3	0.0605
90	92.5	5.3	0.0673
91	92.5	5.3	0.0723
92	92.5	5.3	0.0749
93	92.5	5.3	0.0749
94	92.5	5.3	0.0723
95	92.5	5.3	0.0673
96	92.5	5.3	0.0605
97	92.5	5.3	0.0525
98	92.5	5.3	0.0439
99	92.5	5.3	0.0355
100	92.5	5.3	0.0277
101	92.5	5.3	0.0208
102	92.5	5.3	0.0151

x	μ	σ	Gausian, d = 70 m
80	89	5	0.0158
81	89	5	0.0222
82	89	5	0.0299
83	89	5	0.0388
84	89	5	0.0484
85	89	5	0.0579
86	89	5	0.0666
87	89	5	0.0737
88	89	5	0.0782
89	89	5	0.0798
90	89	5	0.0782
91	89	5	0.0737
92	89	5	0.0666
93	89	5	0.0579
94	89	5	0.0484
95	89	5	0.0388
96	89	5	0.0299
97	89	5	0.0222
98	89	5	0.0158
99	89	5	0.0108
100	89	5	0.0071
101	89	5	0.0045
102	89	5	0.0027

Calculation for Scenario 1 Car 1 Fast fading and shadowing:

While cars are moving one behind another reading taken from each cars										
					Car 1					
d (m)	P_R dBm	PL (dBm)	FSL	shadowing (open area)	Shadowing -FSL	Fast fading	Fast fading (model)	Probability distribution	correction value	log10 correction value
70	-69	79	77.14	79.09	1.95	-0.09	-5.15	0.39	13.17	1.12
64.4	-62	72	76.41	78.88	2.47	-6.88	-4.74	0.41	11.53	1.06
58.85	-66	76	75.63	78.68	3.05	-2.68	-4.33	0.42	10.21	1.01
53.3	-66	76	74.77	78.47	3.70	-2.47	-3.92	0.43	9.15	0.96
47.75	-65	75	73.81	78.27	4.45	-3.27	-3.51	0.42	8.28	0.92
42.2	-61	71	72.74	78.06	5.32	-7.06	-3.11	0.41	7.58	0.88
36.65	-66	76	71.51	77.86	6.34	-1.86	-2.70	0.38	7.02	0.85
31.1	-66	76	70.09	77.65	7.57	-1.65	-2.29	0.35	6.56	0.82
25.55	-70	80	68.38	77.45	9.07	2.55	-1.88	0.30	6.21	0.79
20	-59	69	66.25	77.25	10.99	-8.25	-1.47	0.25	5.94	0.77
2	-62	75	46.25	76.58	30.33	-1.58	-0.15	0.03	5.53	-0.74

Calculation for Scenario 1, car 2 Fast fading and shadowing:

While cars are moving one behind another reading taken from each cars										
							Car 2			
d (m)	P_R dBm	PL dBm	FSL	shadowing (open area)	Shadowing -FSL	Fast fading	Fast fading (model)	Probability distribution	correction value	log10 correction value
70	-70	80	77.14	64.34	-12.80	15.66	-0.0003300	0.0000597	5.53	0.742
64.4	-68	78	76.41	65.30	-11.11	12.70	-0.0002796	0.0000506	5.53	0.742
58.85	-71	81	75.63	66.25	-9.38	14.75	-0.0002297	0.0000415	5.53	0.742
53.3	-71	81	74.77	67.20	-7.56	13.80	-0.0001797	0.0000325	5.53	0.742
47.75	-71	81	73.81	68.15	-5.66	12.85	-0.0001298	0.0000235	5.53	0.742
42.2	-71	81	72.74	69.11	-3.63	11.89	-0.0000798	0.0000144	5.53	0.742
36.65	63	-53	71.51	70.06	-1.46	-123.06	-0.0000299	0.0000054	5.53	0.742
31.1	-79	89	70.09	71.01	0.92	17.99	0.0000201	0.0000036	5.53	0.742
25.55	-70	80	68.38	71.96	3.58	8.04	0.0000701	0.0000127	5.53	0.742
20	-85	95	66.25	72.91	6.66	22.09	0.0001200	0.0000217	5.53	0.742
2	-72	69.3	46.25	76.00	29.75	-6.70	0.0002820	0.0000510	5.53	0.742

Calculation for Scenario 2, car 1:

While cars are moving against another reading from one point										
					Car 1					
d(m)	P_R (dBm)	PL (dBm)	FSL	shadowing (open area)	Shadowing-FSL	Fast fading	Fast fading (model)	Probability distribution	correction value	log10 correction value
64.4	-62	75	76.41	72.08	-4.33	2.92	-4.49	0.42	10.70	1.03
58.85	-66	76	75.63	72.63	-3.00	3.37	-3.15	0.41	7.65	0.88
53.3	-66	77	74.77	73.18	-1.59	3.82	-1.80	0.29	6.15	0.79
42.2	-68	78	72.74	74.28	1.54	3.72	0.89	0.16	5.67	0.75
36.65	-68	78	71.51	74.83	3.31	3.17	2.23	0.34	6.51	0.81
31.1	-60	70	70.09	71.65	1.56	-1.65	3.57	0.43	8.40	0.92
25.55	-61	71	68.38	69.60	1.22	1.40	4.92	0.40	12.20	1.09
20	-61	71	66.25	67.55	1.30	3.45	6.26	0.31	19.93	1.30
2	-60	70	46.25	60.90	14.65	9.10	10.62	0.05	221.27	2.34
64.4	-62	72	76.41	83.95	7.54	-11.95	-4.49	0.42	10.70	1.03
58.85	-66	73	75.63	81.90	6.27	-8.90	-3.15	0.41	7.65	0.88
53.3	-66	74	74.77	79.85	5.08	-5.85	-1.80	0.29	6.15	0.79
42.2	-65	75	72.74	75.75	3.01	-0.75	0.89	0.16	5.67	0.75
36.65	-69	79	71.51	73.70	2.18	5.30	2.23	0.34	6.51	0.81
31.1	-73	83	70.09	71.65	1.56	11.35	3.57	0.43	8.40	0.92
25.55	-66	76	68.38	69.60	1.22	6.40	4.92	0.40	12.20	1.09
20	-77	87	66.25	67.55	1.30	19.45	6.26	0.31	19.93	1.30
2	-60	76	46.25	60.90	14.65	15.10	10.62	0.05	221.27	-2.34

Calculations for Scenario 2, car 2:

					While cars are moving against another reading from one point					
						Car 2				
d(m)	P_R (dBm)	PL (dBm)	FSL	shadowing (open area)	Shadowing-FSL	Fast fading	Fast fading (model)	Probability distribution	correction value	log10 correction value
64.4	-67	77	76.41	84.90	8.49	-7.90	9.15	0.11	85.32	1.93
58.85	-67	77	75.63	84.48	8.85	-7.48	9.38	0.10	98.39	1.99
53.3	-67	77	74.77	84.06	9.29	-7.06	9.62	0.08	113.89	2.06
42.2	-67	77	72.74	83.22	10.48	-6.22	10.09	0.07	154.24	2.19
36.65	-67	77	71.51	82.80	11.28	-5.80	10.32	0.06	180.47	2.26
31.1	-60	70	70.09	71.65	1.56	-1.65	10.56	0.05	211.93	2.33
25.55	-76	86	68.38	69.60	1.22	16.40	10.79	0.04	249.78	2.40
20	-76	86	66.25	67.55	1.30	18.45	11.03	0.04	295.46	2.47
2	-76	86	46.25	60.90	14.65	25.10	11.79	0.02	522.23	2.72
64.4	-76	86	76.41	83.95	7.54	2.05	9.15	0.11	85.32	1.93
58.85	-76	86	75.63	81.90	6.27	4.10	9.38	0.10	98.39	1.99
53.3	-76	86	74.77	79.85	5.08	6.15	9.62	0.08	113.89	2.06
42.2	-76	86	72.74	75.75	3.01	10.25	10.09	0.07	154.24	2.19
36.65	-76	86	71.51	73.70	2.18	12.30	10.32	0.06	180.47	2.26
31.1	-76	86	70.09	71.65	1.56	14.35	10.56	0.05	211.93	2.33
25.55	-76	86	68.38	69.60	1.22	16.40	10.79	0.04	249.78	2.40
20	-60	70	66.25	67.55	1.30	2.45	11.03	0.04	295.46	2.47
2	-60	81.9	46.25	60.90	14.65	21.00	11.79	0.02	522.23	-2.72

Calculation for Scenario 3, Car 1:

					while cars are moving to one point parallelly					
					Car 1					
d(m)	PR (dBm)	PL (dBm)	FSL	shadowing (open area)	Shadowing-FSL	Fast fading	Fast fading (model)	Probability distribution	correction value	log10 correction value
70	-68	78	77.14	72.32	-4.82	5.68	-10.44	0.05	195.65	2.29
64.4	-64	74	76.41	83.95	7.54	-9.95	-8.75	0.13	67.68	1.83
58.85	-71	81	75.63	81.90	6.27	-0.90	-7.08	0.25	28.43	1.45
53.3	-70	80	74.77	79.85	5.08	0.15	-5.40	0.38	14.35	1.16
47.75	-70	80	73.81	77.80	3.99	2.20	-3.72	0.43	8.70	0.94
42.2	-62	72	72.74	75.75	3.01	-3.75	-2.05	0.32	6.34	0.80
36.65	-62	72	71.51	73.70	2.18	-1.70	-0.37	0.07	5.55	0.74
31.1	-62	72	70.09	71.65	1.56	0.35	1.30	0.22	5.85	0.77
25.55	-62	72	68.38	69.60	1.22	2.40	2.98	0.40	7.39	0.87
20	-62	72	66.25	67.55	1.30	4.45	4.66	0.41	11.24	1.05
2	-60	75.3	46.25	60.90	14.65	14.40	10.09	0.07	154.67	-2.19

Calculation for Scenario 3, Car 2:

				while cars are moving to one point parallelly						
					Car 2					
d(m)	PR (dBm)	PL (dBm)	FSL	shadowing (open area)	Shadowing-FSL	Fast fading	Fast fading (model)	Probability distribution	correction value	log10 correction value
70	-69	79	77.14	79.73	2.59	-0.73	-0.002794	0.000505	5.53	0.74
64.4	-70	80	76.41	79.98	3.56	0.02	-0.002570	0.000465	5.53	0.74
58.85	-75	85	75.63	80.22	4.59	4.78	-0.002348	0.000425	5.53	0.74
53.3	-77	87	74.77	80.46	5.70	6.54	-0.002126	0.000384	5.53	0.74
47.75	-67	77	73.81	80.71	6.90	-3.71	-0.001904	0.000344	5.53	0.74
42.2	-79	89	72.74	80.95	8.21	8.05	-0.001682	0.000304	5.53	0.74
36.65	-70	80	71.51	81.20	9.68	-1.20	-0.001460	0.000264	5.53	0.74
31.1	-67	77	70.09	81.44	11.35	-4.44	-0.001238	0.000224	5.53	0.74
25.55	-70	80	68.38	81.68	13.30	-1.68	-0.001016	0.000184	5.53	0.74
20	-66	76	66.25	81.93	15.68	-5.93	-0.000794	0.000144	5.53	0.74
2	-59	81	46.25	82.72	36.47	-1.72	-0.000074	0.000013	5.53	-0.74